Journal of Medicinal Chemistry

Freie Universität Berlin

Subscriber access provided by UB + Fachbibliothek Chemie | (FU-Bibliothekssystem)

Article

# Hydroxypyridinone and 5-aminolaevulinic acid conjugates for photodynamic therapy

Sinan Battah, Robert C. Hider, Alexander J. MacRobert, Paul S. Dobbin, and Tao Zhou

*J. Med. Chem.*, **Just Accepted Manuscript** • Publication Date (Web): 31 Mar 2017

**Downloaded from http://pubs.acs.org on March 31, 2017**

## Just Accepted

"Just Accepted" manuscripts have been peer-reviewed and accepted for publication. They are posted online prior to technical editing, formatting for publication and author proofing. The American Chemical Society provides "Just Accepted" as a free service to the research community to expedite the dissemination of scientific material as soon as possible after acceptance. "Just Accepted" manuscripts appear in full in PDF format accompanied by an HTML abstract. "Just Accepted" manuscripts have been fully peer reviewed, but should not be considered the official version of record. They are accessible to all readers and citable by the Digital Object Identifier (DOI®). "Just Accepted" is an optional service offered to authors. Therefore, the "Just Accepted" Web site may not include all articles that will be published in the journal. After a manuscript is technically edited and formatted, it will be removed from the "Just Accepted" Web site and published as an ASAP article. Note that technical editing may introduce minor changes to the manuscript text and/or graphics which could affect content, and all legal disclaimers and ethical guidelines that apply to the journal pertain. ACS cannot be held responsible for errors or consequences arising from the use of information contained in these "Just Accepted" manuscripts.

ACS Publications

Journal of Medicinal Chemistry is published by the American Chemical Society. 1155 Sixteenth Street N.W., Washington, DC 20036

Published by American Chemical Society. Copyright © American Chemical Society. However, no copyright claim is made to original U.S. Government works, or works produced by employees of any Commonwealth realm Crown government in the course of their duties.

# Hydroxypyridinone and 5-aminolaevulinic acid conjugates for photodynamic therapy

Sinan Battah,[a,c] Robert C. Hider,[b] Alexander J. MacRobert,[c] Paul S. Dobbin,[a] Tao Zhou[d*]

a. School of Biological Sciences, University of Essex, Colchester, CO4 3SQ, UK

b. Division of Pharmaceutical Sciences, King's College London, 150 Stamford Street, London, SE1 9NH, UK

c. Division of Surgery and Interventional Science, University College London, Charles Bell House, 67-73 Riding House Street, London, W1W 7JE, UK

d. School of Food Science and Biotechnology, Zhejiang Gongshang University, Hangzhou, Zhejiang 310018, P. R. China.

ABSTRACT

Photodynamic therapy (PDT) is a promising treatment strategy for malignant and non-malignant lesions. 5-Aminolevulinic acid (ALA) is used as a precursor of the photosensitizer, protoporphyrin IX (PpIX) in dermatology and urology. However, the effectiveness of ALA-PDT is limited by the relatively poor bioavailability of ALA and rapid conversion of PpIX to haem. The main goal of this study was to prepare and investigate a library of single conjugates designed to co-administer the bioactive agents ALA and hydroxypyridinone (HPO) iron chelators. A significant increase in intracellular PpIX levels was observed in all cell lines tested when compared to the administration of ALA alone. The higher PpIX levels observed using the conjugates correlated well with the observed phototoxicity following exposure of cells to light. Passive diffusion appears to be the main mechanism for the majority of ALA-HPOs investigated. This study demonstrates that ALA-HPOs significantly enhance phototherapeutic metabolite formation and phototoxicity.

*KEYWORDS:* Photodynamic Therapy (PDT); 5-aminolaevulinic acid (ALA); iron chelator; hydroxypyridinone (HPO); protoporphyrin IX (PpIX)

## 1. Introduction

Photodynamic therapy (PDT) is based on the activation of exogenously applied or endogenously formed photosensitizers by visible light in the presence of molecular oxygen. Photosensitization results in formation of singlet oxygen, oxidizing cellular macromolecules photochemical reactions, leading to the damage of a variety of subcellular substrates and cell death.[1-4] 5-Aminolaevulinic acid photodynamic therapy (ALA-PDT) utilizes the haem biosynthesis pathway to transiently produce excess (and clinically useful) amounts of the natural endogenous photosensitizer protoporphyrin IX (PpIX). This is achieved by the addition of exogenous ALA, which enters the haem biosynthesis pathway.[5,6] The main advantage of ALA-PDT is the short half-life of its photosensitizing effects, which reduces the duration of skin photosensitivity and its efficacy using topical administration.[7] However, several factors affect ALA-PDT and limit its clinical potential. In particular, the hydrophilic nature of ALA limits its rate of uptake into neoplastic cells and/or penetration into tissue.[8] Considerable efforts have been made recently to overcome the bioavailability limitations associated with ALA, which have mainly been centred on the development of ALA prodrugs with higher lipophilicity, such as esters[7,9-15] and peptide derivatives.[16-18] In simple ester conjugates, ALA is cleaved at the C-terminus *via* interaction with esterases, but in some ALA conjugates cleavage at the N-terminus is also required via peptidases [15,16] and phosphatases.[14] The methyl and hexyl esters of ALA have been approved for topical treatment of basal cell carcinoma in both Europe and Australia. The use of different delivery vehicles, such as microspheres, liposomes, conjugate antibodies, has also been investigated.[19]

The stage following PpIX production in the haem pathway, is the insertion of ferrous iron ($Fe^{2+}$) under the action of the ferrochelatase to convert PpIX into haem.[6] The presence of free

haem acts as a negative feedback mechanism inhibiting ALA synthesis.[6] The exogenous administration of large amounts of ALA bypasses this negative feedback signal.[20] The resultant accumulation of PpIX within the cells is the rate-limiting step for conversion of PpIX to haem by ferrochelatase.[11,21,22] An additional approach to achieve a greater PpIX accumulation involves the chelation of intracellular iron. As a result the conversion of PpIX to haem is decreased, further enhancing the accumulation of PpIX in the cell.[7,8,22] The nonspecific membrane-impermeable metal chelator ethylenediamine tetraacetic acid (EDTA) has been shown to moderately increase PpIX levels in epithelial skin tumors in combination with ALA.[23,24] Desferrioxamine (DFO) is more effective than EDTA at elevating PpIX in cells due to its greater affinity for iron than EDTA.[25-27]

In our studies using 3-hydroxypyridin-4-one chelators (HPO), a combination of ALA and 1,2-diethyl-3-hydroxypyridin-4-one (CP94, **26**) in PDT proved to be an effective technique to increase the efficacy of ALA-PDT within cells *in vitro* and *in vivo*.[28-31] The concept of exploiting high affinity iron(III) chelators for ferrochelatase inhibition in order to increase the ALA-induced PpIX levels is based upon the ability of these compounds to stimulate the oxidation $Fe^{2+}$ to $Fe^{3+}$ at low concentration, with $O_2$ acting as the oxidant. Compound **26** is a member of the hydroxypyridinone family of bidentate iron chelators. It is particularly effective at chelating intracellular iron due to its lower molecular weight and higher lipophilicity than either DFO or EDTA.[32-35] However, co-administration of ALA and iron chelator would be limited by the differing pharmacological properties of the two agents. In contrast, the molecules in which ALA and HPO agents are coupled via cleavable linkages would release the two agents following cellular uptake. The enhanced porphyrin levels would therefore arise principally from simultaneous delivery of the synergistically acting bioactive agents to cell. Indeed, in our

previous work, it has also been demonstrated that some ALA/HPO conjugates are more efficient than ALA and ALA in combination with HPO for PpIX production in some tumor cell lines.[36,37]

Since HPOs, such as **26**, are more effective at chelating intracellular iron than desferrioxamine due to the superior cell membrane permeability of HPOs,[38] in the present work, a range of ALA-HPO conjugates were designed and synthesized in order to synergistically promote intracellular phototoxicity. There is compelling evidence with regards to the important role of the conjugation bonding, the spacers/linkers types, and length of the spacers for ALA-PDT, based on the literature and our previous work.[7,9-13,16,17,36,37] For example, Battah *et al.* found that increasing the linker length in ALA dendritic derivatives led to an enhancement of intracellular porphyrin generation which was ascribed to a reduction in steric hindrance to esterase access.[13] However linkers can also affect the lipophilicity of the conjugate which will in turn affect its bioavailability.[13]

The goal of this investigation was to optimize and determine the efficacy of several spacers that control the PDT of ALA-HPO conjugates. The chosen iron chelators have similar chemical structures to that of 2-ethyl-3-hydroxypyridin-4-one (**26**) attached to ALA *via* a variety of links (Chart 1). The two moieties were covalently bonded through ester bonds, which were predicted to hydrolyze enzymatically under intracellular conditions. The efficacy of these ALA-HPO conjugates has been investigated in various cell lines and the kinetics of PpIX fluorescence and phototoxicity monitored.

## 2. Results and Discussion

### *2.1 Chemistry*

The ability of ALA-HPO conjugates to penetrate the tumour cell membrane and ease of liberating free ALA molecule intracellularly are important factors affecting the activity of the prodrugs. In order to obtain ALA prodrugs with high PpIX generation efficiency and high phototoxicity against tumour cells, a range of ALA-HPO conjugates were designed. (a) HPO has a similar structure to **26**, features a ethyl group at position 2, and is linked to ALA through different lengths of hydrocarbon spacers $(CH_2)_n$, n = 2–12) in compounds (**7a–7f**) *via* readily cleavable ester bond; (b) the same HPO with ethyl group at position 2 is linked to ALA through a triethyleneglycol spacer in compound (**23**); (c) the ethyl group of HPO at position 2 was substituted with 1-hydroxylethyl in compound (**12)** and a methylamino carbonyl group in compound (**18**), and both groups were linked to ALA via ester bonds in these two compounds with a $(CH_2)_6$ hydrocarbon chain; (d) hexyl-ALA and octyl-ALA were chosen for comparison (compounds **24** and **25**), respectively (Chart 1).

**Preparation of ALA-HPO conjugates 7.** The synthetic route of ALA-HPO conjugates **7** starting from ethyl maltol (**1a**) is outlined in Scheme 1. The benzylation of ethyl maltol with benzyl chloride provided **2a** in 66% yield. The amino alcohol spacers **3a**, **3b** and **3c** (n=2, 4 and 6, respectively) are commercially available, whereas **3d**, **3e** and **3f** (n=8, 10 and 12, respectively) were synthesized by the Mitsunobu reaction using triphenylphosphine ($Ph_3P$), phthalimide and diisopropyl azodicarboxylate (DIPAD), followed by hydrazination. Condensation of **2a** and amino alcohol **3** under alkaline condition provided the 2-alkyl-substituted 3-hydroxypyridin-4-ones (**4**). The protected pyridinones **4** were coupled with *N*-Cbz ALA, which was prepared in aqueous solution at pH 8-10 at room temperature in reasonable yield, forming an ester link using the standard coupling agents 1,3-dicyclohexylcabodiimide (DCC) and 4-dimethylaminopyridine (DMAP), yielding the protected ALA-HPO conjugates **6**. Deprotection of **6** was achieved by

hydrogenation at 40 psi $H_2$ atmosphere in methanol and ethyl acetate (1:3, by volume) in the presence of benzyl chloride to afford the hydrochlorides of ALA-HPO conjugates **7**. The clogP values of this series **7a-7f** range from -1.96 to 0.91 (Table 1).

**Preparation of ALA-HPO conjugates 12 and 18.** The synthetic route of ALA-HPO conjugate **12** is presented in Scheme 2. Conversion of the 2-ethyl group of **2a** to 2-hydroxyethyl was accomplished using selenium oxide as a oxidizing agent in phenyl bromide with reflux, providing compound **8** in 43 % yield; at the same time, another oxidized product 2-acetyl-3-(benzyloxy)-4*H*-pyran-4-one was detected (11 % yield). The newly formed hydroxyl group in compound **8** was subsequently protected using benzyl bromide in a two-phase reaction using tetrabutylammonium sulfate as phase transfer catalyst, yielding **9** in 62 % yield. Compound **9** was converted to the pyridinone **10** *via* condensation with 6-amino-hexan-1-ol. Conversion of **10** to **12** was achieved using the similar procedures to that for ALA-HPO conjugates **7** (Scheme 2). The synthesis of ALA-HPO conjugate **18** using maltol (**1b**) as a starting material is shown in Scheme 3. The methyl group in benzyl protected maltol was selectively oxidized by selenium oxide to form an aldehyde **13**, which was further oxidized to a carboxylic acid **14** in the presence of sodium hypochlorite and sulfamic acid.[39] The carboxyl group was activated by DCC/*N*-hydroxysuccimide (NHS) to form an activated ester, which was subsequently coupled to methylamine, providing a pyranone derivative **15**. Insertion of the amino alcohol spacers into the pyranone ring was achieved by refluxing the corresponding spacer with **15** in an alcoholic solution of sodium hydroxide at pH 12 to afford the pyridinone **16,** which was coupled to *N*-Cbz ALA, providing **17**, the latter was subjected to hydrogenation, generating the ALA-HPO conjugate **18** (Scheme 3). The two conjugates **12** and **18** are relatively hydrophilic, the clog*P* values being -1.28 and -1.65 respectively (Table 1).

**Preparation of the triethylene glycol-linked ALA-HPO conjugate 23.** The amino alcohol **20** was prepared from triethylene glycol using the Mitsunobu reaction (Scheme 4). Condensation of **20** with the benzyl protected ethyl maltol (**2a**) yielded the derivative **21**. Conjugation with protected ALA using similar methods to that described for the hydrocarbon linked molecule (**4**) yielded the desired ester (**22**), which upon hydrogenation yielded the ALA-HPO conjugate (**23**) (Scheme 4). This is the most hydrophilic compound of the series with a clog*P* value of -2.37 (Table 1).

### *2.2 Biological evaluation*

MCF-7 cells (human breast adenocarcinoma) and MCF-7R cells (doxorubicin resistant subline, MCF-7/DXR) were chosen to assess the efficacy of the newly synthesized ALA–HPO conjugates to generate the photoactive, fluorescent photosensitizer PpIX. PDT has been proposed in several studies as an alternative in overcoming multidrug resistance (MDR) phenotype.[10,40]

Therefore, the goal was to compare the accumulation and photosensitization of PpIX in MCF-7 human breast adenocarcinoma cells and its doxorubicin MDR resistant counterpart, which is characterized by the overexpression of P-gp. Human KB cells were also selected, which are derived from an oral epidermal squamous cell carcinoma of the mouth. ALA has been used for head and neck cancer, both topically and with oral administration.[41,42]

#### *2.2.1 Concentration dependence profile*

The fluorescence intensity of PpIX generated in MCF-7R cells after exposure of ALA or HPO-ALA conjugates for 6 h is presented in **Figure 1**. Fluorescence spectra were consistent with the production of PpIX, and the peak emission at 635 nm was recorded for each compound. The protophyrin PpIX fluorescence induced by exposure to the majority of ALA-HPO

conjugates indicated an efficient internalization and metabolism within all the investigated cell lines. PpIX production exhibited a dose dependent response for all ALA-HPO single conjugates. Porphyrin generation was enhanced over a range of concentrations between (1–100 μM) after 6 h incubation for the compounds with long hydrocarbon spacers between ALA and HPO with the ethyl group at position 2 (**Figure 1**). PpIX generation was elevated significantly from **7b** (n = 4 clog*P* -1.42) to **7f** (n = 12, clog*P* 0.91) by factor of about 2-25, reaching the maximum level with compound **7e** (n = 10), while compound **7a** failed to increase PpIX greatly as compared to that produced with ALA itself at the highest concentration (100 μM). This effect is attributed to the graduation of lipophilicity and the changes in steric hindrance around the ester hydrolysis sites.[12] The presence of the HPO moiety within the conjugates enhanced the fluorescence intensities for **7c**, **7d**, and **7e** compounds when compared with those of compounds **24** and **25,** having same esters **(**hexyl and octyl ALA esters).[43] The ALA-HPO featuring the triethylene glycol spacer **23** with a clog*P* value of -2.37 elevated PpIX production levels to over 20 fold higher than ALA at 100μM. PpIX accumulation induced by HPOs with the side chain, 2-ethyl (compound **7c**) was superior to those HPOs with the modified side groups (hydroxyethyl and amido -$CONHCH_3$) of compounds **12** and **18**, respectively. Although, compounds **7c, 12,** and **18** were linked to ALA *via* the same spacers $(CH_2)_6$, compound **7c** produced PpIX fluorescence >15 fold that of ALA, compound **12** yielded >10 fold, while compound **18** failed to enhance the level of PpIX production with respect to PpIX-ALA.

### *2.2.2 Fluorescence kinetics*

ALA-HPOs single conjugates were clearly more efficient than ALA with respect to PpIX generation over an incubation period up to 24 h in KB cell lines (**Figures 2**). PpIX fluorescence

kinetics of ALA-HPOs with long hydrocarbon spacers, (**7d, 7e** and **7f**) continued to exhibit significant enhancement in PpIX generation over time.

The compounds with longer hydrocarbon spacers, demonstrated efficient PpIX production which was further enhanced by the presence of HPO (with a similar structure to **26**) over incubation time ranging between 2 h and 24 h (**Figure 2**). The existence of HPO at the other end of the spacers (n =6, n =8, n =10) probably led to a reduction of the toxicity of the spacers on ester formation with ALA. On the other hand HPO could boost the penetration of conjugates through the cell membrane. ALA esters with hydrocarbons over n = 6 have reduced bioavailabilities as a result of being trapped within bilayers.[11,12,44] There have been many reports detailing the mechanistic uptake of ALA and ALA esters, which showed that the mechanism of uptake of ALA is *via* active transport and its esters adopt a passive diffusion pathway.[7,9-12]

We have compared the production of PpIX in the KB cell line at 37 °C and 4 °C to investigate whether ALA and ALA-HPOs are transported into the cell primarily by active and passive transport mechanisms, respectively. An active transport system would be significantly inhibited by lowering the temperature to 4 °C, whereas involvement of passive transport would still enable uptake at lower temperatures. The results presented in **Figure 3** show that incorporation of ALA and ALA-HPOs into KB cells is temperature dependent: i.e. when ALA-HPOs uptake was measured at 4 °C, a marginal reduction of PpIX fluorescence was observed, up to ≈ 5% for most of ALA-HPOs, except PpIX generated by **12** which impaired by ca. ≈ 50%. In contrast PpIX fluorescence produced by ALA was found to be significantly reduced up to 90%, which is in good agreement with previous studies.[45] Thus, we can conclude that an incorporation of ALA and ALA-HPOs into the KB cells (and by extrapolation the MCF-7 and MCF7R cell lines also) involves two different mechanistic pathways, with passive diffusion predominating as

the main pathway for ALA-HPOs single conjugates.

A comparison of PpIX fluorescence kinetics produced upon a 24 h time-course treatment of compounds **7c**, **12** and **18** highlighted the significant role of the HPO in PpIX production (each compound contained a hexyl linker to ALA but different structures of HPO). Compound **12** exhibited higher porphyrin fluorescence levels than **7c**, while compound **18** was not effective at enhancing PpIX accumulation. Surprisingly, the hydrophilic conjugate **23,** with a triethylenglycol spacer, was found to be highly effective in all cell lines, particularly at longer time points (**Figures 1**, **2** and **4**).

For compounds **7**, there is a clear relationship between the length of the hydrocarbon linkers and PpIX accumulation (**Figures 1**, **2** and **4**), the effect increasing over the range n=2 to n=10, whereas with n=12 a relative decline was found in PpIX accumulation probably due to the relatively low solubility of this compound. The optimum compound (**7e**) has a clog*P* value of 0.73. The compounds **7d**, **7e**, **7f** and **23** are all more effective than the hexyl- and octyl esters of ALA (**24** and **25**) (**Figure 1**).

The length of the hydrocarbon link is also directly correlated with the clog*P* values, and in view of their molecular size and range of clog*P* values, it is most probable that they gain access to the cytoplasm of cells by non-facilitated diffusion.[12] However the high efficiency of **23** (clog*P* = -2.37) would indicate that this molecule is a substrate for transport, a possibility, which is currently under investigation.

Although co-administration of ALA and HPOs separately (ie without conjugation) was found to enhance PpIX levels when compared to ALA alone, the additive effect was significantly weaker than when the related conjugates were investigated as shown in **Figure 4**. This

corresponds well with our previous studies in cells using co-incubation of ALA and **26**.[27] The use of **26** in combination with ALA and methyl ALA ester also produced significant enhancements of PpIX fluorescence in human glioma cells. At the highest concentrations of each prodrug, **26** enhanced PpIX fluorescence significantly at 3 h for ALA and by more than 50% at 6 h for ALA methyl ester. In our study, an increase in PpIX levels by approximately a factor of two was observed in both MCF-7 and MCF-7R cell lines in the presence of the conjugates when compared to the equivalent separate additions after 6 h incubation (**Figure 4A**). The synergistic effect on PpIX enhancement was also confirmed in KB cells over a 24 h time course study, employing ALA-HPO conjugates compared to co-administered ALA and HPOs. There were 2-3 fold increases in PpIX production as a result of ALA-HPO conjugate incubation over the co-administered ALA and HPOs as a mixture, particularly at the longer incubation times of 6 and 24 h (**Figure 4B**).

ALA-HPO conjugates developed in the present investigation were found to be more effective in PpIX production than our previously reported compounds, in which ALA moiety was coupled to HPO moiety *via* an amide linkage.[37] For instance, after incubation with KB cells for 24h, conjugates **7d**, **7e** and **7f** (50μM) could produce PpIX level with 8, 10.2 and 9.2 fold higher than ALA; whereas the best compound in the previous study could only generate 2.9 fold higher porphyrin levels than ALA.[37] This is probably due to the fact that esterase activity in cells is relatively high, thus rapidly generating free ALA and HPO, while peptidase activity in cells is at a relatively lower level. The relative solubility of the compounds in the cell culture medium with the ester linkage was much higher than with the amide linkage, which may also have adversely affected the efficiency of the amide compounds.

Uehlinger et al. investigated ALA and a range of ALA esters (methyl, ethyl, butyl, hexyl,

octyl and cyclo-hexyl esters) for the efficacy in producing PpIX in some tumour cell lines (A549, T24, J82 and BEAS-2B cells), and found that in most cell lines ALA hexyl ester showed the most efficient PpIX formation.[11] Wu et al. also demonstrates that the cellular PpIX content in 1 mM ALA incubated nasopharyngeal carcinoma (NPC) cells is similar to that in 0.03 mM ALA hexyl ester incubated cells, reflecting that ALA hexyl ester is more efficient than ALA for inducing PpIX production.[41] However in the present study, compounds **7c**, **7d**, **7e** and **7f** were demonstrated to be even more efficient in PpIX formation than the ALA hexyl ester (**24**) (Figure 1).

Intracellular PpIX fluorescence of PAM212 keratinocyte cells has been reported to be enhanced by a factor of 5 after 6 h incubation with 0.01 mM of an ALA-peptide conjugate, Ac-*L*-Phe-ALA-OMe, compared with ALA at the same concentration, where the amino acid is conjugated at the N-terminus of ALA.[16] More extensive investigation of peptide prodrugs of ALA (Ac-Xaa-ALA-OR, where Xaa is an α-amino acid) indicated that some of the peptide prodrugs are more efficient in inducing PpIX accumulation than ALA in PAM212 and also A549 and Caco-2 cell lines.[17] For instance, at 0.1 mM, after incubation with PAM212 keratinocyte cells for 6h, peptide prodrugs Ac-*L*-Leu-ALA-OMe, Ac-*L*-Phe-ALA-OMe, Ac-*L*-GluOBu-$^{t}$-ALA-OMe and Ac-*L*-Phe-Met-OMe could produce PpIX level with 7.5, 4.4, 6.5 and 5.9 fold higher than ALA.[17]

Recently, Babič et al. have reported that two ALA hexyl ester analogues, P-ALA-Hex and PSI-ALA-Hex, which were obtained by modification of the *N*-terminus amino group, displayed reduced acute toxicity compared to the ALA hexyl ester with superior dose response profiles of protoporphyrin IX synthesis and fluorescence intensity in human glioblastoma cells *in vitro*.[14]

### *2.2.3 Phototoxicity studies*

The phototoxicity of ALA and ALA-HPO conjugates, incubated with tumor cells for 4h and irradiated with blue light (2.5 J/cm$^2$), was investigated over a range of concentrations between 2-100 μM. The data for KB cells are presented in **Figure 5**. The percentages of cell survival with respect to control cells (without compounds) were calculated for various concentrations of investigated compounds. In agreement with the data from the PpIX fluorescence experiments, the ALA-HPO conjugates that exhibited a marked enhancement of PpIX fluorescence also exhibited high phototoxicity. In general, compounds **7c, 7d, 7e, 7f** and **23** were found to be the most phototoxic compounds at low concentrations.

The $LD_{50}$ values (at 2.5 J/cm$^2$), calculated from **Figure 5** are presented in Table 1. The values for **7d, 7e** and **7f** are between 2.3 μM and 12.9 μM for all investigated cell lines, in contrast to the much higher value of 100 μM for ALA. For **23**, the $LD_{50}$ values were somewhat higher, ranging between 11.3 and 19.6 μM. The $LD_{50}$ value of the hexyl ester of ALA (**24**) was found to be similar to that of **7e.** Again, ALA-HPO conjugates in the present investigation were more phototoxic upon exposure to light than our previously reported compounds. For instance, after the incubation of KB cells with **1d**, **1e** and **1f** (10μM), followed by illumination, the survival percentages of KB cells were under 6%; while the survival percentages of KB cells incubated with the previously reported best ALA-HPO compound (200 μM) was 7.8%.[37] The results of phototoxicity of ALA-HPO conjugates were in accordance with those of relative PpIX generation.

Phototoxicity was both drug concentration and irradiation dose dependent. Our results for the ALA hexyl ester are in accord with previous studies. For example, the hexyl ester was much

more phototoxic than ALA against nasopharyngeal carcinoma (NPC) cells.[41] To achieve an 80% death rate ($LD_{80}$), 0.75 mM ALA and 6 J/cm$^2$ light dose were required, while only 0.03 mM ALA hexyl ester and 4 J/cm$^2$ light dose were needed. In terms of overall photodynamic dose, the ALA hexyl ester is about 40 times more potent than ALA in cell inactivation.[41] Although, iron can affect the generation of ROS through redox processes, the high production of PpIX through the use of HPOs and improved PDT potency may predominate over any secondary factors related to the ability of iron to catalyze ROS generation/cascades following PpIX-induced PDT. Moreover despite the reduction of iron availability, thereby increasing PpIX accumulation, other transition metals and freshly released labile iron may preserve the ROS cascades *via* Fenton reactions.[46]

### *2.2.4 Cell viability and dark toxicity*

The "dark" toxicity (namely, the cytotoxicity in the absence of irradiation) of the ALA-HPOs conjugates was also evaluated in the KB cells (**Figure 6**). The data indicated that there was no appreciable toxicity found for ALA or all the investigated compounds at 200 μM after 4h or 24 h incubation.

The structural conjugates, where ALA is at one end and HPO moieties on the other end of the spacers, do not appear to induce significantly higher dark toxicity than ALA itself. In contrast, ALA ester derivatives, i.e., hexyl-ALA (**24**) and octyl-ALA (**25)** showed significant dark toxicity (9% and 14% cell survival, respectively at the lower concentration of 100 μM after 4h of incubation. The incubation of ALA-HPO conjugates for 24h did not affect the cell viability more than a 4h incubation. However, almost no cells survived after 24h incubation with hexyl-ALA

and octyl-ALA. It also appears with this assay that HPOs with the spacers n = 6 or more elicit no chemical toxicity to the cells after cleavage and releasing ALA. The much lower dark toxicity of the HPO conjugate, albeit in a tumour cell line is a significant finding in respect to the prodrug metabolism, particularly, if it is to be considered for systemic administration, however further in vivo studies will be required to validate lower dark toxicities.

### *2.2.5 Intracellular Prodrug Quantitative Determination*

The cellular uptake of the prodrugs and their intracellular conversion to ALA was assessed by quantitative determination of ALA using a HPLC-based fluorescence method. We adopted a previously reported derivatization method.[17,45,47,48] A higher accumulation of ALA was observed after 2h incubation at 100 μM particularly in KB and MCF-7R cells using the conjugates **(Figure 7A)**. For example, six and eight-fold enhancements with **7d** and **7e** was observed with respect to ALA itself. These results were largely reflected in the intracellular PpIX levels measured at 24h following 2h incubation by fresh medium without ALA or prodrugs (**Figure 7B)**.

The fluorescence intensity of PpIX in MCF-7R, which is a chemotherapy resistant breast cancer tumour cell line, elicited higher porphyrin levels than in the MCF-7 non-resistant counterpart, for the majority of ALA-HPO compounds. Malik and co-workers have also demonstrated that MCF-7R, doxorubicin resistant tumour cells, are capable of producing higher levels of porphyrins than sensitive MCF-7 cells due to the low expression of the enzyme ferrochelatase in combination with high mitochondrial activity.[40] As found in the present study, higher PpIX levels than the doxorubicin sensitive MCF-7 cells were also observed.

## 3. Conclusions

ALA-PDT provides a promising therapy for many types of cancer, but it is important to improve its efficiency when ALA is administered systemically and intravenously in order to overcome inefficient cell uptake and conversion to PpIX. Iron chelating agents have been demonstrated to be effective at improving ALA-PDT by increasing the cellular PpIX accumulation. In the present study, a series of ALA-HPO conjugates were synthesized and tested in three cells lines. All ALA-HPO conjugates showed significantly elevated cellular PpIX accumulation in KB, MCF-7 and MCF-7R cell lines when compared to ALA and a combination of ALA with the corresponding HPO. Overall, compound **7e,** with a linker of $(CH_2)_{10}$, was found to be the most effective in both enhancement of cellular PpIX levels and tumour cell phototoxicity, with comparable efficacy to the ALA hexyl ester.

## 4. Experimental Section

### *4.1 General*

$^{1}H$ and $^{13}C$ NMR were recorded on a Jeol EX270 MHz spectrometer (Jeol Ltd, Toxyo, Japan), or on Bruker Avance 400 or Bruker Avance 500 spectrometer. Chemical shifts are quoted in ppm measured downfield relative to TMS. Ultraviolet-visible spectra were recorded on a Unicam UV2 spectrometer (Perkin-Elmer, Beaconsfield, UK) in dichloromethane solution. Infrared spectra were recorded on a Nicolet FTIR (Fourier Transform Infrared Spectroscopy) spectrometer (Thermo-Electro Corporation, Wisconsin, USA) as thin films in dichloromethane. Mass spectra were obtained using a EI/CI (Electroionization/Chemical Ionization). Analytical thin layer chromatography was carried out using Adsorbentien, aluminium-backed, silica-coated plates (VWR, Germany) which were visualized using ultraviolet light (254nm). Column

chromatography was carried out using Alfa Aester silica gel (220-440 mesh flash grade). High Performance Liquid Chromatography (HPLC) was performed on a Si (55w) 250  2.1 mm column attached to a Agilent instrument (Agilent, Life Sciences & Chemical Analysis Group, UK). All the chemicals were purchased from Aldrich, Fisher, Alfa Aester and Aladdin**,** and used without further purification unless otherwise stated. Analytical analysis was carried out by Electrospray (ES) instrument (Quattro Premier XE, Micromass Technologies) which coupled to high performance liquid chromatograpy (HPLC, Waters/AcQuity Ultrapreformance LC, Waters, Manchester, UK). Electrospray ionization (ESI) mass spectra were obtained by infusing samples into an LCQ Deca XP ion trap instrument. High resolution mass spectra (HRMS) were determined on Waters QTOF micro. The purity of ALA-HPO conjugates was determined by analytical HPLC (Agilent system 1100) coupled with UV−vis/DAD (diode array detector) using C18 reverse-phase column [HYPERSIL (5 μm, 2.1 mm × 150 mm)]. The total run was monitored with UV detector at two wavelengths 268 and 282 nm. The purities of all the AlA-HPO conjugates were over 95%.

### *4.2 Synthetic Procedures*

#### *4.2.1 N-Benzyloxycarbonyl-5-aminolevulinic acid (N-Cbz ALA)*

5-Aminolaevulinic acid (0.22 g, 1.30 mmol) was dissolved in water (3mL) and the solution was adjusted to pH 8-10 with sodium carbonate solution. *N*-Benzyloxycarbonyl chloride (0.30 mL, 1.40 mmol) was dissolved in dioxane (3mL) and added to the mixture.  After 18 h at room temperature the solvents were removed in vacuum and 0.1M of sodium hydroxide (20mL) was added. The mixture was washed with diethyl ether three times. The aqueous layer was

neutralized to pH 6 and the product was extracted with dichloromethane (5×20mL). The organic layers were combined, dried with $Na_2SO_4$ and evaporated to yield the product as thick oil (0.18 g, 52%). $^1$H NMR (270 MHz, $CDCl_3$) δ 2.73 (m, 4H, $CH_2$), 4.10 (s, 2H, $CH_2$), 5.12 (s, 2H, $CH_2$), 5.45 (br, 1H, NH), 7.31 (m, 5H, Ph); $^{13}$C NMR (67.5 MHz, $CDCl_3$) δ 27.02, 34.20, 46.61, 65.54, 71.33, 127.66, 127.86, 128.94, 138.31, 155.00, 171.82. ESI-MS: *m/z* 264 ($[M-H]^-$).

*4.2.2 3-(Benzyloxy)-2-ethyl-4H-pyran-4-one (**2a**)*

To a solution of ethyl maltol (84g, 0.6mol) in methanol (300 mL) was added NaOH solution (26.4g in 80 mL $H_2O$). The mixture was heated to reflux and benzyl bromide (85.6 mL, 0.72mol) was added dropwise over a 2h period. The solution was maintained at 60-65 $^o$C overnight. NaBr was removed by filtration and the filtrate was concentrated. Dichloromethane (400mL) was added to the residue, and washed with 5% NaOH solution (3×250mL), $H_2O$ (2×300mL) and dried over anhydrous $Na_2SO_4$. After removal of the solvent, diethyl ether (100mL) was added to the residue and allowed to stand to 4 $^o$C. The product was obtained as white crystals (91.2g, 66 %). $^1$H NMR ($CDCl_3$, 400MHz) δ 0.98 (t, *J* = 7.6Hz, 3H, $CH_3$), 2.50 (q, *J* = 7.6Hz, 2H, $CH_2$), 5.17 (s, 2H, $CH_2$), 6.37 (d, *J* = 5.6Hz, 1H, C5-H in pyridinone), 7.30-7.41 (m, 5H, Ph), 7.63 (d, *J* = 5.6Hz, 1H, C6-H in pyridinone). ESI-MS: *m/z* 231 ($[M+H]^+$).

*4.2.3 General synthetic procedure for amino alcohols (**3**)*

*8-Aminooctan-1-ol* (**3d**): To a mixture of 1,8-octanediol (13.3g, 91mmol), phthalimide (8.92g, 60.6mmol), triphenylphosphine (15.89g, 60.6 mmol) in tetrahydrofuran (THF) (150mL), cooled on an ice-bath, was added dropwise diisopropyl azodicarboxylate (DIPAD) (12.25g, 60.0mmol) over a period of 1 h. The mixture was stirred at room temperature overnight. After removal of the solvent, the residue was purified by column chromatography using ethyl acetate/cyclohexane

(1:2) as an eluent to obtain 2-(8-hydroxyoctyl)isoindoline-1,3-dione (**3d'**) as a white solid (13.2g, 79%). $^1$H NMR ($CDCl_3$, 400MHz) δ1.32 (m, 8H, $CH_2$), 1.53 (m, 2H, $CH_2$), 1.65 (m, 2H, $CH_2$), 3.61 (t, *J* = 6.5Hz, 2H, $CH_2$), 3.66 (t, *J* = 7.5Hz, 2H, $CH_2$), 7.69 (m, 2H, Ph), 7.82 (m, 2H, Ph). ESI-MS: *m/z* 276 ($[M + H]^+$), 298 ($[M + Na]^+$).

To a solution of **3d'** (12.5g, 45.5mmol) in 95% ethanol (150mL) was added 50% hydrazine (4.35g in 15mL $H_2O$, 68.2mmol). The mixture was refluxed for 3 h, and then 10M HCl (15mL) was added. Reflux was continued for a further 15min, cooled with an ice-bath and then filtered. The filtrate was concentrated, and 15 mL of water was added, washed with diethyl ether. The aqueous layer was adjusted to pH 12 with 10 M NaOH, and then extracted with dichloromethane (5×120mL). The combined organic layer was dried over anhydrous $Na_2SO_4$. After removal of the solvent, 8-aminooctan-1-ol (**3d**) was obtained as a white solid (5.41g, 82%).$^1$H NMR ($CDCl_3$, 500MHz) δ1.32 (m, 8H, $CH_2$), 1.45 (m, 2H, $CH_2$), 1.56 (m, 2H, $CH_2$), 2.58 (t, *J* = 7.0Hz, 2H, $CH_2$), 2.68 (t, *J* = 7.0Hz, 2H, $CH_2$), 3.63 (t, *J* = 6.5Hz, 2H, $CH_2$). ESI-MS: *m/z* 146 ($[M + H]^+$).

*2-(10-hydroxydecyl)isoindoline-1,3-dione* (**3e'**): $^1$H NMR ($CDCl_3$, 500MHz) δ1.25 (m, 10H, $CH_2$), 1.31 (m, 2H, $CH_2$), 1.55 (m, 2H, $CH_2$), 1.66 (m, 2H, $CH_2$), 3.63 (t, *J* = 6.5Hz, 2H, $CH_2$), 3.67 (t, *J* = 7.5Hz, 2H, $CH_2$), 7.70 (m, 2H, Ph), 7.83 (m, 2H, Ph). ESI-MS: *m/z* 304 ($[M + H]^+$), 326 ($[M + Na]^+$).

*10-Aminodecan-1-ol* (**3e**): $^1$H NMR ($CDCl_3$, 500MHz) δ1.28 (m, 10H, $CH_2$), 1.42 (m, 4H, $CH_2$), 1.55 (m, 2H, $CH_2$), 2.67 (t, *J* = 7.0Hz, 2H, $CH_2$), 3.62 (t, *J* = 6.5Hz, 2H, $CH_2$). ESI-MS: *m/z* 174 ($[M + H]^+$).

2-(12-hydroxydodecyl)isoindoline-1,3-dione (**3f'**):$^1$H NMR ($CDCl_3$, 500MHz) δ1.26 (m, 16H, $CH_2$), 1.32 (m, 2H, $CH_2$), 1.66 (m, 2H, $CH_2$), 3.63 (t, *J* = 6.5Hz, 2H, $CH_2$), 3.67 (t, *J* = 7.5Hz, 2H, $CH_2$), 7.70 (m, 2H, Ph), 7.84 (m, 2H, Ph). ESI-MS: *m/z* 332 ($[M + H]^+$), 354 ($[M + Na]^+$).

12-aminododecan-1-ol (**3f**): $^1$H NMR ($CDCl_3$, 500MHz) δ1.27 (m, 16H, $CH_2$), 1.43 (m, 2H, $CH_2$), 1.55 (m, 2H, $CH_2$), 2.67 (t, *J* = 7.0Hz, 2H, $CH_2$), 3.62 (t, *J* = 6.5Hz, 2H, $CH_2$). ESI-MS: *m/z* 202 ($[M + H]^+$).

*4.2.4 General synthetic procedure for hydroxypyridinones (4)*

*3-(Benzyloxy)-2-ethyl-1-(2-hydroxyethyl)pyridin-4(1H)-one* (**4a**)*:* Compound **2a** (4.6g, 20 mmol) was dissolved in ethanol (30mL)/$H_2O$(30mL), followed by the addition of ethanolamine (3.05g, 50mmol) and 2M NaOH solution (2mL). The mixture was refluxed for 18h. After cooling to room temperature, the solution was adjusted to pH 1 with concentrated hydrochloric acid, and then concentrated to half volume. 50 mL of $H_2O$ was added. The solution was washed with diethyl ether (2×50mL), adjusted to pH 9 with 10 M NaOH, extracted with DCM (3×50mL). The combined organic layers were dried over anhydrous $Na_2SO_4$. After removal of the solvent, **4a** was obtained by crystallization from ethyl acetate as yellow crystals (4.06g, 74%). $^1$H NMR ($CDCl_3$, 400MHz) δ 0.96 (t, *J* = 7.6Hz, 3H, $CH_3$), 2.68 (q, *J* = 7.6Hz, 2H, $CH_2$), 3.86 (m, 2H, $CH_2$), 3.90 (m, 2H, $CH_2$), 5.06 (s, 2H, $CH_2$), 6.15 (d, *J* = 7.4Hz, 1H, C5-H in pyridinone), 7.30-7.40 (m, 4H, Ph and buried C6-H in pyridinone), 7.42 (m, 2H, Ph). ESI-MS: *m/z* 274 ($[M + H]^+$), 296 ($[M + Na]^+$).

*3-(Benzyloxy)-2-ethyl-1-(4-hydroxybutyl)pyridin-4(1H)-one* (**4b**): 69% yield. $^1$H NMR ($CDCl_3$, 400MHz) δ 1.02 (t, *J* = 7.6Hz, 3H, $CH_3$), 1.54 (m, 2H, $CH_2$), 1.78 (m, 2H, $CH_2$), 2.57 (q, *J* = 7.6Hz, 2H, $CH_2$), 3.66 (t, *J* = 6.0Hz, 2H, $CH_2$), 3.82 (t, *J* = 7.6Hz, 2H, $CH_2$), 5.22 (s, 2H, $CH_2$),

6.36 (d, *J* = 7.6Hz, 1H, C5-H in pyridinone), 7.25 (d, *J* = 7.6Hz, 1H, C6-H in pyridinone), 7.28-7.35 (m, 3H, Ph), 7.41 (m, 2H, Ph); ESI-MS: *m/z* 302 ($[M + H]^+$), 324 ($[M + Na]^+$).

*3-(Benzyloxy)-2-ethyl-1-(6-hydroxyhexyl)pyridin-4(1H)-one* (**4c**): 79% yield. $^1$H NMR ($CDCl_3$, 400MHz) δ 1.03 (t, *J* = 7.6Hz, 3H, $CH_3$), 1.30-1.44 (m, 4H, $CH_2$), 1.56 (m, 2H, $CH_2$), 1.67 (m, 2H, $CH_2$), 2.56 (q, *J* = 7.6Hz, 2H, $CH_2$), 3.64 (t, *J* = 6.4Hz, 2H, $CH_2$), 3.75 (t, *J* = 7.6Hz, 2H, $CH_2$), 5.26 (s, 2H, $CH_2$), 6.41 (d, *J* = 7.6Hz, 1H, C5-H in pyridinone), 7.18 (d, *J* = 7.6Hz, 1H, C6-H in pyridinone), 7.27-7.35 (m, 3H, Ph), 7.42 (m, 2H, Ph); ESI-MS: *m/z* 330 ($[M + H]^+$), 352 ($[M + Na]^+$).

*3-(Benzyloxy)-2-ethyl-1-(8-hydroxyoctyl)pyridin-4(1H)-one* (**4d**): 67% yield. $^1$H NMR ($CDCl_3$, 400MHz) δ 1.03 (t, *J* = 7.6Hz, 3H, $CH_3$), 1.32 (m, 8H, $CH_2$), 1.56 (m, 2H, $CH_2$), 1.66 (m, 2H, $CH_2$), 2.57 (q, *J* = 7.6Hz, 2H, $CH_2$), 3.64 (t, *J* = 6.6Hz, 2H, $CH_2$), 3.74 (t, *J* = 7.6Hz, 2H, $CH_2$), 5.28 (s, 2H, $CH_2$), 6.43 (d, *J* = 7.6Hz, 1H, C5-H in pyridinone), 7.17 (d, *J* = 7.6Hz, 1H, C6-H in pyridinone), 7.29-7.35 (m, 3H, Ph), 7.43 (m, 2H, Ph). ESI-MS: *m/z* 358 ($[M + H]^+$), 380 ($[M + Na]^+$).

*3-(Benzyloxy)-2-ethyl-1-(10-hydroxydecyl)pyridin-4(1H)-one* (**4e**): 63% yield. $^1$H NMR ($CDCl_3$, 500MHz) δ 1.04 (t, *J* = 7.5Hz, 3H, $CH_3$), 1.29 (m, 10H, $CH_2$), 1.55 (m, 2H, $CH_2$), 1.66 (m, 4H, $CH_2$), 2.57 (q, *J* = 7.5Hz, 2H, $CH_2$), 3.64 (t, *J* = 6.5Hz, 2H, $CH_2$), 3.74 (t, *J* = 7.5Hz, 2H, $CH_2$), 5.29 (s, 2H, $CH_2$), 6.42 (d, *J* = 7.5Hz, 1H, C5-H in pyridinone), 7.17 (d, *J* = 7.5Hz, 1H, C6-H in pyridinone), 7.29-7.35 (m, 3H, Ph), 7.44 (m, 2H, Ph). ESI-MS: *m/z* 386 ($[M + H]^+$), 408 ($[M + Na]^+$).

*3-(Benzyloxy)-2-ethyl-1-(12-hydroxydodecyl)pyridin-4(1H)-one* (**4f**): 62% yield. $^1$H NMR ($CDCl_3$, 500MHz) δ 1.04 (t, *J* = 7.5Hz, 3H, $CH_3$), 1.28 (m, 16H, $CH_2$), 1.55 (m, 2H, $CH_2$), 1.66

(m, 2H, $CH_2$), 2.57 (q, $J$ = 7.5Hz, 2H, $CH_2$), 3.64 (t, $J$ = 6.5Hz, 2H, $CH_2$), 3.74 (t, $J$ = 7.5Hz, 2H, $CH_2$), 5.28 (s, 2H, $CH_2$), 6.42 (d, $J$ = 7.5Hz, 1H, C5-H in pyridinone), 7.17 (d, $J$ = 7.5Hz, 1H, C6-H in pyridinone), 7.29-7.35 (m, 3H, Ph), 7.43 (m, 2H, Ph). ESI-MS: *m/z* 414 ($[M + H]^+$), 436 ($[M + Na]^+$).

### *4.2.5 General procedure for ALA coupling to pyridinones*

*N*-Benzyloxycarbonyl-5-aminolevulinic acid (2.2 mmol) was dissolved in DCM (20 mL) and DMF (5mL) under argon, DCC (2 mmol) and DMAP (0.2 mmol). The mixture was left to stir for 50 min at room temperature. Compound **4** (2 mmol) was dissolved in DCM (10mL) and added dropwise over 30min. The mixture was stirring overnight at room temperature. The heavy precipitate was filtered off and the solvents were evaporated *in vacuo*. The residue was dissolved in DCM and washed with water then saturated sodium hydrogen carbonate. The solvent was removed and the residue was purified by flash chromatography on silica gel using a gradient of petroleum ether/ethyl acetate (1:4), followed by 100% ethyl acetate and then methanol/ethyl acetate (1:9). The products **6** were isolated as yellow pastes with yields of 72-80%.

*2-(3-(Benzyloxy)-2-ethyl-4-oxopyridin-1(4H)-yl)ethyl-5-(((benzyloxy)carbonyl)amino)-4-oxopentanoate **(6a)**:* Yield 77%. $^1$H NMR ($CDCl_3$, 270MHz) δ 0.95 (t, $J$ = 7.6Hz, 3H $CH_3$), 2.47 (m, 2H, $CH_2$), 2.55 (m, 2H, $CH_2$), 2.59 (q, $J$ = 7.6Hz, 2H, $CH_2$), 3.95 (m, 4H, $CH_2$), 4.12 (s, 2H, $CH_2$), 5.01 (s, 2H, $CH_2$), 5.14 (s, 2H, $CH_2$), 6.30 (s, 1H, NH), 6.32 (*d*, *J*= 7.4, 1H, C5-H in pyridinone), 7.2-7.36 (m, 11H, 10H from 2Ph and 1H from C6-H in pyridinone); $^{13}$C NMR: δ 13.2, 17.7, 27.7, 34.5, 49.9, 50.6, 62.6, 66.8, 71.7, 117.2, 123.3, 127.9, 128.1, 128.3, 128.6, 128.7, 136.1, 138.5, 142.0, 142.4, 146.2, 156.2, 173.1, 173.5, 206.7. ESI-MS: *m/z* 521 ($[M + H]^+$), 543 ($[M + Na]^+$).

*4-(3-(Benzyloxy)-2-ethyl-4-oxopyridin-1(4H)-yl)butyl-5-(((benzyloxy)carbonyl)amino)-4-oxopentanoate (**6b**):* Yield 79%. $^1$H NMR ($CDCl_3$, 270MHz): 0.95 (t, $J$ = 7.6Hz, 3H $CH_3$), 1.52 (m, 2H, $CH_2$), 1.67 (m, 2H, $CH_2$), 2.47 (m, 2H, $CH_2$), 2.49 (m, 2H, $CH_2$), 2.52 (q, $J$ = 7.6Hz, 2H, $CH_2$), 3.63 (m, 2H, $CH_2$), 3.93 (m, 4H, $CH_2$), 4.98 (s, 2H, $CH_2$), 5.11 (s, 2H, $CH_2$), 6.01 (s, 1H, NH), 6.31 (d, $J$ = 7.4, 1H, C5-H in pyridinone), 7.19-7.22 (m, 11H, 10H from 2Ph and 1H from C6-H in pyridinone). $^{13}$C NMR: δ13.3, 25.7, 26.3, 27.9, 28.5, 29.1, 31.5, 50.7, 53.3, 64.8, 66.9, 72.9, 76.8, 117.4, 127.9, 128.1, 128.2, 128.3, 128.6, 128.7, 136.2, 138.5, 145.2, 156.3, 172.5, 173.4, 204.0. ESI-MS: *m/z* 549 ($[M+H]^+$). 571 ($[M+Na]^+$).

*6-(3-(Benzyloxy)-2-ethyl-4-oxopyridin-1(4H)-yl)hexyl-5-(((benzyloxy)carbonyl)amino)-4-oxopentanoate (**6c**):* Yield 80%. $^1$H NMR ($CDCl_3$, 270MHz): δ 0.98 (t, $J$ = 7.6Hz, 3H, $CH_3$), 1.21-1.23 (m, 4H, $CH_2$), 1.52-1.55(m, 4H, $CH_2$), 2.44–2.47 (m, 4H, $CH_2$), 3.63 (q, $J$ = 7.4Hz, 2H, $CH_2$), 3.84-3.98 (m, 6H, $CH_2$), 5.01 (s, 2H, $CH_2$), 5.11 (s, 2H, $CH_2$), 6.02( br, 1H, NH), 6.31 (d, $J$ = 7.4, 1H, C5-H in pyridinone), 7.18 (d, $J$ = 7.4Hz, C6-H in pyridinone), 7.21 (m, 10H, Ph); $^{13}$C NMR: δ 13.9, 19.5, 25.7, 26.7, 27.5, 28.9, 29.2, 29.3, 29.4, 31.7, 34.5, 49.9, 50.7, 52.6, 65.0, 67.0, 71.2, 117.5 127.9, 128.2, 128.8 136.4, 138.1, 138.5, 142.0, 156.2, 172.5, 173.1, 206.7. ESI-MS: *m/z* 577 ($[M+H]^+$), 599 ($[M+Na]^+$).

*8-(3-(Benzyloxy)-2-ethyl-4-oxopyridin-1(4H)-yl)octyl 5-(((benzyloxy)carbonyl)amino)-4-oxopentanoate (**6d**):* Yield 75%: $^1$H NMR ($CDCl_3$, 270MHz): δ 1.02 (t, $J$ = 7.6Hz, 3H, $CH_3$), 1.29 (m, 8H, $CH_2$), 1.63(m, 4H, $CH_2$), 2.55–2.70 (m, 6H, $CH_2$), 3.75 (m 2H, $CH_2$), 4.03–4.13(m, 4H, $CH_2$), 5.09 (s, 2H, $CH_2$), 5.25 (s, 2H, $CH_2$), 5.57( br, 1H, NH), 6.49 (d, 1H, $J$= 7.4Hz, 1H, C5-H in pyridinone), 7.28–7.64(m, 11H, 2Ph and C6-H in pyridinone); $^{13}$C NMR: δ13.4, 20.2, 25.9, 26.5, 27.9, 28.2, 28.6, 29.2, 29.3, 29.4, 31.5, 50.7, 53.3, 64.8, 67.0, 72.9, 117.5, 127.9, 128.1, 128.3, 128.5, 128.6, 128.8, 134.2, 137.9, 138.1, 146.8, 156.3, 172.6, 173.6, 204.1. ESI-

MS: m/z, 605 ($[M+H]^+$), 627 ($[M+Na]^+$).

*10-(3-(Benzyloxy)-2-ethyl-4-oxopyridin-1(4H)-yl)decyl 5-(((benzyloxy)carbonyl)amino)-4-oxopentanoate (**6e**):* Yield 72%. $^1$H NMR ($CDCl_3$, 270MHz): δ 1.02 (t, *J* = 7.6Hz, 3H, $CH_3$), 1.24 (m, 12H, $CH_2$), 1.56 (m, 4H, $CH_2$), 2.51-2.66 (m, 6H, $CH_2$), 3.7 (m, 2H, $CH_2$), 4.01-4.09 (m, 4H, $CH_2$), 4.95 (s, 2H, $CH_2$), 5.23 (s, 2H, $CH_2$), 5.69 (br, 1H, NH), 6.36 (d, *J*= 7.4, 1H, C5-H in pyridinone), 7.12 (d, *J*= 7.4, 1H, C6-H in pyridinone), 7.26-7.31 (m, 10H, Ph); $^{13}$CNMR: 13.4, 20.3, 25.9, 26.5, 27.3, 27.9, 28.2, 28.6, 28.9, 29.2, 29.3, 29.4, 31.5, 50.7, 53.3, 64.8, 67.0, 72.9, 117.5, 127.9, 128.1, 128.3, 128.5, 128.6, 128.8, 134.2, 137.9, 138.1, 146.2, 156.3, 172.6, 173.6, 204.1. ESI-MS: *m/z* 633 ($[M+H]^+$), 655 ($[M+Na]^+$).

*12-(3-(Benzyloxy)-2-ethyl-4-oxopyridin-1(4H)-yl)dodecyl 5-(((benzyloxy)carbonyl)amino)-4-oxopentanoate (**6f**):* Yield 73%. $^1$H NMR ($CDCl_3$, 270MHz) 0.98 (t, *J* = 7.6Hz, 3H, $CH_3$), 1.03 (m, 16H, $CH_2$), 1.57-1.60 (m, 4H, $CH_2$), 2.53–2.64 (m, 6H, $CH_2$), 3.71 (q, *J*=7.4Hz, 2H, $CH_2$), 4.02 (m, 2H, $CH_2$), 4,11 (s, 2H, $CH_2$), 5.06 (s, 2H, $CH_2$), 5.24 (s, 2H, $CH_2$), 5.59 (br, 1H, NH), 6.40 (d, *J* = 7.4Hz, 1H, C5-H in pyridinone), 7.28 (d, *J* = 7.4Hz, 1H, C6-H in pyridinone), 7.30–7.39 (m, 10H, Ph); $^{13}$C NMR: 13.3, 20.1, 25.9, 26.4, 27.6, 28.2, 28.6, 28.9, 29.2, 29.4, 29.5, 29.7, 31.6, 50.7, 53.3, 60.5, 65.0, 67.0, 72.9, 117.5, 128.8, 127.9, 128.1, 128.2, 128.6, 128.8, 136.5, 137.9, 138.7, 145.6, 156.3, 172.5, 173.6, 204.1. ESI-MS: *m/z* 661 ($[M+H]^+$), 683 ($[M+Na]^+$).

### *4.2.6 General procedure for the deprotection of amino and hydroxyl groups of ALA-HPO conjugates*

Compounds **6a**–**6f, 11, 17** and **22** (1 equiv.) were dissolved in methanol/ethyl acetate (50mL, 1:4). Catalytic amount of palladium on carbon (5% Pd/C, 10% weight of protected ALA-HPO conjugates) and benzyl chloride (2.2 equiv.) were added. The hydrogenation was carried out

under 40 psi $H_2$ at room temperature for 10 min. Pd/C was filtered off and the filtrate was evaporated to dryness. The residues were purified by semi-preparative Agilent HPLC using revers-phase Waters column (4.6mm X 250 mm) eluted with acetonitrile/methanol (30:70, V/V) with flow rate 1mL/min. AlA-HPO conjugates **7, 12, 18** and **23** were isolated as thick oils. The purity of all compounds was determined by analytical HPLC (Agilent system 1100) coupled with UV−vis/DAD using C18 reverse-phase column [HYPERSIL (5 μm, 2.1 mm × 150 mm)]. The mobile phase was A (0.1% TFA in MeOH:$H_2O$, 2:98), 100% isocratic for 5 min, B (0.1% TFA in MeOH:$H_2O$, 98:2), gradient from 0-50% between 6-10 min, 50% B isocratic from 11-15 min, then equilibrate with 100% A for 2 min. The total elution time was 18 min and flow rate was 0.25 mL/min. The total run was monitored with UV detector at two wavelengths 268 and 282 nm.

*(2-(2-Ethyl-3-hydroxy-4-oxopyridin-1(4H)-yl)ethoxy)-2,5-dioxopentan-1-aminium chloride* (**7a**): The product was isolated as thick oil, yield 35%, HPLC-DAD ($R_t$: 2.3 min; purity 95.6%) $^1$H NMR (DMSO, 270MHz): 1.23 (t, $J$ = 7.5Hz, 3H, $CH_3$), 2.64 (m, 2H, $CH_2$), 2.85 (m, 2H, $CH_2$), 3.06 (m, 2H, $CH_2$), 3.59 (m, 2H, $CH_2$), 4.02 (s, 2H, $CH_2$), 4.38 (m, 2H, $CH_2$), 7.13 (d, $J$=6.7Hz, 1H, C5-H in pyridinone), 7.66 (m, 3H, $H_3N^+$), 8.10 (d, $J$ = 6.9Hz, 1H, C6-H in pyridinone); $^{13}$C NMR: δ12.1, 15.3, 27.7, 36.2, 44.3, 53.7, 55.5, 113.3 127.9, 134.0, 143.0, 164.9, 172.1, 206.2. ESI-MS: *m/z* 297 ($[M+H]^+$); HRMS: HRMS: Calcd. for $C_{14}H_{21}N_2O_5$:, 297.1450 ($[M+H]^+$), found: 297.1441.

*5-(4-(2-Ethyl-3-hydroxy-4-oxopyridin-1(4H)-yl)butoxy)-2,5-dioxopentan-1-aminium chloride* (**7b**): Yield 42%, HPLC-DAD ($R_t$: 3.2 min; purity 96.3%). $^1$H NMR ($CD_3OH$, 270MHz): δ 1.26 (t, $J$ = 7.1Hz, 3H, $CH_3$), 1.82 (m, 2H, $CH_2$) 1.98 (m, 2H,$CH_2$), 2.64 (m, 2H, $CH_2$), 2.83 (m, 2H, $CH_2$), 3.06 (q, $J$ = 5.4Hz, 2H, $CH_2$), 4.09 (m, 4H, $CH_2$), 4.43 (m, 2H, $CH_2$), 7.12 (d, $J$ = 6.4Hz, 1H, C5-H in pyridinone), 8.32 (d, $J$ = 6.7Hz, 1H, C6-H in pyridinone); $^{13}$C NMR: δ 11.1, 15.3,

19.4, 26.8, 27.1, 36.2, 50.3, 52.6, 64.4, 116.8, 126.2, 137.4, 140.5, 156.2, 172.2, 201.2. ESI-MS: *m/z* 325 ($[M+H]^+$), 347 ($[M+Na]^+$); HRMS: Calcd for $C_{16}H_{25}N_2O_5$:, 325.1763 ($[M+H]^+$), found: 325.1743.

*5-((6-(2-Ethyl-3-hydroxy-4-oxopyridin-1(4H)-yl)hexyl)oxy)-2,5-dioxopentan-1-aminium chloride* (**7c**)**:** Yield 42%, HPLC-DAD ($R_t$: 3.7 min; purity 96.6%). $^1$H NMR ($CD_3OH$, 270MHz): δ 1.29 (t, $J$ = 7.1Hz, 3H, $CH_3$), 1.45 (m, 4H, $CH_2$) 1.89 (m, 4H, $CH_2$), 2.67 (m, 4H, $CH_2$), 2.82 (m, 2H, $CH_2$), 3.29 (m, 2H, $CH_2$), 3.55 (m, 2H, $CH_2$), 4.06 (m, 2H, $CH_2$), 7.15 (d, $J$ = 6.4Hz, 1H, C5-H in pyridinone), 8.20 (d, $J$ = 6.7Hz, 1H, C6-H in pyridinone); $^{13}$C NMR: δ 11.1, 15.2, 19.4, 25.4, 26.8, 29.1, 34.2, 36.2, 50.3, 52.6, 64.4, 111.9 136.4, 138.5, 156.2, 172.2, 173.1, 201.2. ESI-MS: *m/z* 353.3 ($[M+H]^+$), 375.3 ($[M+Na]^+$); HRMS: Calcd for $C_{18}H_{29}N_2O_5$:, 353.2076 ($[M+H]^+$), found: 353.2065.

*5-((8-(2-Ethyl-3-hydroxy-4-oxopyridin-1(4H)-yl)octyl)oxy)-2,5-dioxopentan-1-aminium) dichloride* (**7d**)**:** Yield 48%, HPLC-DAD ($R_t$: 4.3 min; purity 97.7%). $^1$H NMR ($CD_3OH$, 270MHz): δ 1.17 (t, 3H, $J$ = 7.1Hz, $CH_3$), 1.26 (m, 12H, $CH_2$), 2.66 (m, 2H, $CH_2$), 2.85 (m, 2H, $CH_2$), 3.49 (m, 2H, $CH_2$), 3.61, (m, 2H, $CH_2$), 4.05-4.11 (m, 4H, $CH_2$), 7.33 (d, $J$ = 6.4Hz, 1H, C5-H in pyridinone) 8.22 (d, $J$ = 6.7Hz, 1H, C6-H in pyridinone); $^{13}$C NMR: δ 11.3, 19.9, 25.7, 26.4, 29.0, 29.1, 31.3, 34.2, 36.2, 50.3, 52.6, 64.4, 110.8 138.4, 143.4, 146.4, 158.4, 172.9, 201.7. ESI-MS: *m/z* 382.1 ($[M+H]^+$), 404.2 ($[M+Na]^+$). HRMS: Calcd. for $C_{20}H_{33}N_2O_5$:, 381.2389 ($[M+H]^+$), found: 381.2383.

*5-((10-(2-Ethyl-3-hydroxy-4-oxopyridin-1(4H)-yl)decyl)oxy)-2,5-dioxopentan-1-aminium chloride* (**7e**)**:** Yield 45%, HPLC-DAD ($R_t$: 5.4 min; purity 97.4%). $^1$H NMR ($CD_3OH$, 270MHz): δ 1.17 (t, $J$ = 7.1Hz, 3H, $CH_3$), 1.26 (m, 16H, $CH_2$), 2.66 (m, 2H, $CH_2$), 2.85 (m, 2H,

$CH_2$), 3.15 (m, 2H, $CH_2$), 3.91 (m, 2H, $CH_2$), 4.05 (s, 2H, $CH_2$), 4.60 (m, 2H, $CH_2$), 7.15 (d, $J$ = 6.4Hz, 1H, C5-H in pyridinone), 8.20 (d, $J$ = 6.7Hz, 1H, C6-H in pyridinone); $^{13}$C NMR: δ 11.3, 19.8, 25.0, 26.4, 29.0, 29.1, 29.3, 31.2, 34.2, 50.3, 52.6, 56.4, 61.7, 64.7, 110.8, 138.4, 143.5, 146.0, 158.2, 172.9, 201.2. ES-MS: 409.2 ($[M+H]^+$); HRMS: Calcd for $C_{22}H_{37}N_2O_5$:, 409.2702 ($[M+H]^+$), found: 409.2700.

*5-((12-(2-Ethyl-3-hydroxy-4-oxopyridin-1(4H)-yl)dodecyl)oxy)-2,5-dioxopentan-1-aminium chloride* (**7f**): Yield 43%, HPLC-DAD ($R_t$: 6.2 min; purity 96.8%). $^1$H NMR ($CD_3OH$, 270MHz): δ 1.11 (t, $J$ = 7.1Hz, 3H, $CH_3$), 1.13 (m, 20H, $CH_2$), 2.66 (m, 2H, $CH_2$), 2.90 (m, 2H, $CH_2$), 3.32 (m, 2H, $CH_2$), 3.91 (m, 2H, $CH_2$), 4.09 (s, 2H, $CH_2$), 4.60 (m, 2H, $CH_2$), 7.33 (d, $J$ = 6.4Hz, 1H, C5-H in pyridinone), 8.22 (d, $J$ = 6.7Hz, 1H, C6-H in pyridinone); $^{13}$C NMR: δ 11.3, 19.8, 25.7, 26.1, 28.7, 28.9, 29.0, 29.1, 29.3, 31.3, 32.4, 34.2, 50.2, 52.3, 56.4, 61.7, 64.7, 110.7, 138.1, 143.5, 146.4, 158.4, 172.9, 201.2. ESI-MS: *m/z* 437.0 ($[M+H]^+$), 459.1 ($[M+Na]^+$); HRMS: Calcd for $C_{24}H_{41}N_2O_5$:, 437.3015 ($[M+H]^+$), found: 437.3025.

### *4.2.7 Synthesis of ALA-HPO conjugate 12*

*3-(Benzyloxy)-2-(1-hydroxyethyl)-4H-pyran-4-one (**8**)*: A mixture of 3-(benzyloxy)-2-ethyl-4H-pyran-4-one (**2a**) (10g, 43.4mmol), $SeO_2$ (14.5g, 130.4mmol) and phenyl bromide (50mL) was heated to 135-140$^o$C with vigorous stirring for 4h. After filtration, the filtrate was concentrated and the residue was purified by column chromatography using ethyl acetate/cycle hexane (2:1) as an eluent to obtain product as a brown oil (4.6g, 43%). $^1$H NMR ($CDCl_3$, 400MHz) δ 1.23 (d, $J$ = 6.7Hz, 3H, $CH_3$), 4.85 (q, $J$ = 6.7Hz, 1H, CH), 5.22 (d, $J$ = 2.0Hz, 2H, $CH_2$), 6.46 (d, $J$ =

5.6Hz, 1H, C5-H in pyridinone), 7.37 (m, 5H, Ph), 7.71 (d, *J* = 5.6Hz, 1H, C6-H in pyridinone). ESI-MS: *m/z* 247 ($[M + H]^+$).

*3-(Benzyloxy)-2-(1-(benzyloxy)ethyl)-4H-pyran-4-one (**9**)*: To a solution of 3-(benzyloxy)-2-(1-hydroxyethyl)-4H-pyran-4-one (**8**) (4.0g, 16.2mmol) in dichloromethane (50mL) was added 50% KOH (5.45g, 48.6mmol) and $Bu_4N^+HSO_4^-$ (0.1g). The mixture was stirred at room temperature for 30 min before benzyl bromide (4.17g, 24.4mmol) was added dropwise. The reaction was monitored by TLC until the starting material disappeared. The reaction mixture was washed with brine, and the organic layer was dried over anhydrous $Na_2SO_4$. After removal of the solvent, the residue was purified by column chromatography using ethyl acetate/cycle hexane (1:2) as an eluent to obtain product **9** as a pale yellow oil (3.4g, 62%). $^1$H NMR ($CDCl_3$, 400MHz) δ 1.14 (d, *J* = 6.6Hz, 3H, $CH_3$), 4.19-4.28 (m, 2H, $CH_2$), 4.67 (q, *J* = 6.6Hz, 1H, CH), 5.19 (s, 2H, $CH_2$), 6.40 (d, *J* = 5.6Hz, 1H, C5-H in pyridinone), 7.24-7.33 (m, 10H, Ph), 7.71 (d, *J* = 5.6Hz, 1H, C6-H in pyridinone). ESI-MS: *m/z* 337 ($[M + H]^+$).

*3-(Benzyloxy)-2-(1-(benzyloxy)ethyl)-1-(6-hydroxyhexyl)pyridin-4(1H)-one (**10**)*: The synthetic procedure was similar to that adopted for the preparation of **4**. Yield: 66%. $^1$H NMR ($CDCl_3$, 400MHz) δ 1.14-1.29 (m, 4H, $CH_2$), 1.22 (d, *J* = 7.0Hz, 3H, $CH_3$), 1.44 (m, 2H, $CH_2$), 1.62 (m, 2H, $CH_2$), 3.56 (t, *J* = 6.5Hz, 2H, $CH_2$), 3.98 and 4.10 (m, 2H, $CH_2$), 4.16 (s, 2H, $CH_2$), 5.26 (s, 2H, $CH_2$), 6.48 (d, *J* = 7.5Hz, 1H, C5-H in pyridinone), 7.21 (m, 3H, Ph and buried C6-H in pyridinone), 7.28-7.34 (m, 8H, Ph). ESI-MS: *m/z* 436 ($[M + H]^+$), 458 ($[M + Na]^+$).

*6-(3-(Benzyloxy)-2-(1-(benzyloxy)ethyl)-4-oxopyridin-1(4H)-yl)hexyl-5-((benzyloxycarbonyl)amino)-4-oxopentanoate* (**11**): $^1$H NMR ($CDCl_3$, 270MHz) δ 1.22 (m, 7H, $2CH_2$ and $CH_3$), 1.44-1.59 (m, 4H, $2CH_2$), 2.58-2.69 (m, 4H, $2CH_2$), 3.93-4.14 (m, 7H, $3CH_2$ and

CH), 5.09(s, 2H, $CH_2$), 5.22 (s, 4H, $2CH_2$), 5.63 (s, 1H, NH), 6.46 (d, *J*= 7.4Hz, 1H, C5-H in pyridinone), 7.38-7.47(m, 15H, 3Ph), 8.82 (d, *J*= 7.4Hz, 1H, C6-H in pyridinone); $^{13}$C NMR: δ 20.4, 25.6, 26.2, 27.7, 27.8, 28.4, 31.7, 34.5, 50.7, 52.3, 64.6, 66.7, 67.0, 69.7, 71.2, 74.7, 117.9, 127.6, 128.2, 128.3, 128.5, 128.5, 129.4, 137.5, 138.5, 140.0, 144.5, 146.0, 156.3, 172.5, 173.8, 206.7. ESI-MS: *m/z* 683 ($[M+H]^+$), 705 ($[M+Na]^+$).

*5-((6-(2-Ethyl-3-hydroxy-4-oxopyridin-1(4H)-yl)hexyl)oxy)-2,5-dioxopentan-1-aminium chloride* (**12**)**:** The product was isolated as thick oil, yield 35%, HPLC-DAD ($R_t$: 3.5 min; purity 96.5%). $^1$H NMR ($CD_3OH$, 270MHz): δ 1.20-1.44 (m, 7H, $2CH_2$ and $CH_3$), 1.93-2.06 (m, 4H, $CH_2$), 2.66 (m, 2H, $CH_2$), 2.81 (m, 2H, $CH_2$), 3.57 (m, 2H, $CH_2$), 4.09 (m, 4H, $2CH_2$), 5.67 (m, 1H, CH), 7.19 (d, *J* = 6.4Hz, 1H, C5-H in pyridinon), 8.21 (d, *J* = 6.7Hz, 1H, C6-H in pyridinon); $^{13}$C NMR: δ 13.9, 19.4, 25.4, 26.8, 27.1, 34.23, 36.2, 50.3, 52.6, 64.4, 72.2, 116.8, 126.2, 137.4, 141.5, 156.2, 173.1, 201.2. ESI-MS: 369.2 ($[M+H]^+$), 391.2 ($[M+Na]^+$); HRMS: Calcd for $C_{18}H_{29}N_2O_6$:, 369.2026 ($[M+H]^+$), found: 369.2019.

### *4.2.8 Synthesis of ALA-HPO conjugate 18*

*3-(Benzyloxy)-N-methyl-4-oxo-4H-pyran-2-carboxamide (**15**):* A solution of 3-(benzyloxy)-4-oxo-4H-pyran-2-carboxylic acid **14** (0.94g, 3.82mmol) and *N*-hydroxysuccimide (0.485g, 4.2mmol) in tetrahydrogenfuran (20mL) was stirred at room temperature for 30min. DCC (0.866g, 4.2mmol) was added, the stirring was continued for 5h. Methylamine (2M in THF, 4.58mmol) was added, and the solution was stirred at room temperature overnight. After filtration, the filtrate was concentrated and the residue was purified by column chromatography using ethyl acetate/methanol (9:1) as an eluent to obtain product (0.85g, 86%). $^1$H NMR ($CDCl_3$, 400MHz) δ 2.78 (d, *J* = 5.0Hz, 3H, $CH_3$), 5.39 (s, 2H, $CH_2$), 6.49 (d, *J* = 5.6Hz, 1H, C5-H in

pyridinone), 7.40 (m, 5H, Ph), 7.70 (br, 1H, NH), 7.84 (d, $J$ = 5.6Hz, 1H, C6-H in pyridinone). ESI-MS: *m/z* 260 ($[M+H]^+$).

*3-(Benzyloxy)-1-(6-hydroxyhexyl)-N-methyl-4-oxo-1,4-dihydropyridine-2-carboxamide* ***(16)***: $^1$H NMR ($CDCl_3$, 400MHz) δ1.30-1.42 (m, 4H, $CH_2$), 1.55 (m, 2H, $CH_2$), 1.76 (m, 2H, $CH_2$), 2.73 (d, $J$ = 4.9Hz, 3H, $CH_3$), 3.62 (t, $J$ = 6.3Hz, 2H, $CH_2$), 3.83 (t, $J$ = 7.5Hz, 2H, $CH_2$), 5.09 (s, 2H, $CH_2$), 6.30 (d, $J$ = 7.4Hz, 1H, C5-H in pyridinone), 7.13 (d, $J$ = 7.4Hz, 1H, C6-H in pyridinone), 7.31 (m, 5H, Ph), 7.43 (m, 1H, NH). ESI-MS: *m/z* 359 ($[M + H]^+$), 381 ($[M + Na]^+$).

*6-(3-(Benzyloxy)-2-(methylcarbamoyl)-4-oxopyridin-1(4H)-yl)hexyl 5-(((benzyloxy)carbonyl)amino)-4-oxopentanoate* ***(17)***: The product was isolated as yellow paste, yield 80%. $^1$H NMR ($CDCl_3$, 270MHz): δ 1.30 (m, 4H, $2CH_2$), 1.57 (m, 2H, $CH_2$), 1.74 (m, 2H, $CH_2$), 2.60–2.68 (m, 4H, $2CH_2$), 2.70 (d, $J$ = 2.9Hz, 3H, $CH_3$), 2.76 (m, 2H, $CH_2$) 4.02 (m, 4H, $2CH_2$), 4.98 (s, 2H, $CH_2$), 5.06 (s, 2H, $CH_2$), 5.71 (br, 1H, NH), 6.20 (d, $J$ = 7.4, 1H, C5-H in pyridinone), 7.25 (d, $J$ = 7.4Hz, C6-H in pyridinone), 7.27–7.32 (m, 10H, 2Ph), 8.01 (br, H, NH); $^{13}$C NMR: δ 25.1, 25.4, 26.0, 26.3, 27.9, 28.4, 31.7, 34.5, 50.1, 54.9, 64.6, 67.7, 74.2, 118.0, 128.0, 128.1, 128.3, 128.6, 134.9, 136.8, 138.5, 140.1, 145.8, 156.2, 161.6, 172.5, 173.8, 204.3. ESI-MS: *m/z* 606 ($[M+H]^+$), 628 ($[M+Na]^+$).

*5-((6-(3-Hydroxy-2-(methylcarbamoyl)-4-oxopyridin-1(4H)-yl)hexyl)oxy)-2,5-dioxopentan-1-aminium chloride* (**18**): The product was isolated as thick oil, yield 37%, HPLC-DAD ($R_t$: 3.4 min; purity 97.0%). $^1$H NMR ($CD_3OH$, 270MHz): δ 1.52 (m, 4H, $2CH_2$), 1.64 (m, 2H, $CH_2$), 2.07 (m, 2H, $CH_2$), 2.67 (m, 2H, $CH_2$), 2.83 (m, 2H, $CH_2$), 3.28 (s, 3H, $CH_3$), 4.02-4.07 (m, 4H, $2CH_2$), 4.35 (m, 2H, $CH_2$), 7.26 (d, $J$ = 6.4Hz, 1H, C5-H in pyridinone), 8.30 (d, $J$ = 6.7Hz, 1H, C6-H in pyridinone); $^{13}$C NMR: δ 25.0, 25.5, 26.1, 27.2, 27.9, 28.1, 34.0, 50.1, 59.2, 64.6, 112.0,

136.5, 138.7, 143.0, 162.5, 158.2, 172.8, 201.8. ESI-MS: *m/z* 382.2 ($[M+H]^+$), 404.4 ($[M+Na]^+$); HRMS: Calcd for $C_{18}H_{28}N_3O_6$:, 382.1978 ($[M+H]^+$), found: 382.1966.

### *4.2.9 Synthesis of ALA-HPO conjugate 23*

*2-(2-(2-Aminoethoxy)ethoxy)ethanol (**20**):* The synthetic procedure was similar to that of **3**. $^1$H NMR ($CDCl_3$, 400MHz) δ2.19 (br, 2H, $NH_2$), 2.88 (t, *J* = 5.1Hz, 2H, $CH_2$), 3.55 (t, *J* = 5.1Hz, 2H, $CH_2$), 3.60-3.74 (m, 8H, $CH_2$). ESI-MS: *m/z* 150 ($[M+H]^+$).

*1-(2-(2-Hydroxyethoxy)ethyl)-3-(benzyloxy)-2-ethylpyridin-4(1H)-one (**21**)*: The synthetic procedure was similar to that of **4**. $^1$H NMR ($CDCl_3$, 400MHz) δ1.00 (t, *J* = 7.5Hz, 3H, $CH_3$), 2.63 (q, *J* = 7.5Hz, 2H, $CH_2$), 3.54 (m, 6H, $CH_2$), 3.66-3.73 (m, 4H, $CH_2$), 3.98 (t, *J* = 5.2Hz, 2H, $CH_2$), 5.25 (s, 2H, $CH_2$), 6.43 (d, *J* = 7.6Hz, 1H, C5-H in pyridinone), 7.28-7.35 (m, 4H, Ph and buried C6-H in pyridinone), 7.44 (m, 2H, Ph). ESI-MS: m/z 362 ($[M + H]^+$), 384 ($[M + Na]^+$).

*2-(2-(2-(3-(Benzyloxy)-2-ethyl-4-oxopyridin-1(4H)-yl)ethoxy)ethoxy)ethyl-5-(((benzyloxy)carbonyl)amino)-4-oxopentanoate (**22**)*: The product was isolated as thick oil, yield 70%. $^1$H NMR ($CDCl_3$, 270MHz) δ 0.98 (t, 3H, $CH_3$), 2.59-2.61 (m, 6H, $3CH_2$), 3.47-3.73 (m, 8H, $4CH_2$), 3.90 (m, 2H, $CH_2$), 4.04 (s, 2H, $CH_2$), 4.30 (m, 2H, $CH_2$), 5.05 (s, 2H, $CH_2$), 5.19 (s, 2H, $CH_2$), 5.90 (br, H, NH), 6.35 (d, 1H, *J*= 7.4Hz, 1H, C5-H in pyridinone), 7.23-7.27 (m,10H, 2Ph), 7.38 (d, *J* = 7.4Hz, 1H, C6-H pyridinone); $^{13}$C NMR: δ 13.2, 19.5, 27.5, 27.9, 34.2, 50.7, 52.6, 63.8, 70.6, 70.9, 71.3, 72.9, 117.1, 128.3, 128.7,136.5, 137.9, 138.0, 139.4, 145.7, 146.0, 156.5, 172.4, 173.7, 204.6. ESI-MS: *m/z* 609 ($[M+H]^+$), 631 ($[M+Na]^+$).

*5-(2-(2-(2-(2-Ethyl-3-hydroxy-4-oxopyridin-1(4H)-yl)ethoxy)ethoxy)ethoxy)-2,5-dioxopentan-1-aminium chloride (**23**)*: The product was isolated as thick oil, yield 37%, HPLC-DAD ($R_t$: 2.8 min; purity 95.8%). $^1$H NMR ($CD_3OH$, 270MHz): δ 1.17 (t, *J* = 7.1Hz, 3H, $CH_3$), 2.56 (m, 2H,

$CH_2$), 2.73 (m, 2H, $CH_2$), 3.01 (q, $J$ = 5.4Hz, 2H, $CH_2$), 3.21 (m, 2H, $CH_2$), 3.47 (m, 6H, $3CH_2$), 3.54 (m, 2H, $CH_2$), 3.90 (s, 2H, $CH_2$), 4.65 (m, 2H, $CH_2$), 7.07 (d, $J$ = 6.4Hz, 1H, C5-H in pyridinon), 8.08 (d, $J$ = 6.7Hz, 1H, C6-H in pyridinone); $^{13}$C NMR: δ13.9, 19.4, 25.4, 27.1, 34.23, 36.2, 26.8, 50.3, 52.6, 64.4, 72.2, 116.8 126.2, 137.4, 141.5.4, 156.2, 173.1, 204.2. ESI-MS: *m/z* 385 ($[M+H]^+$), 407 ($[M+Na]^+$); HRMS: Calcd for $C_{18}H_{29}N_2O_7$:, 385.1975 ($[M+H]^+$), found: 385.1968.

### 4.3 Cell Culture

The human breast adenocarcinoma cell line MCF-7, doxorubicin-resistant counterpart MCF-7R line (were donated by Dr Marilena Loizidou, UCL) and the human oral epidermal carcinoma KB cell line was purchased from ATCC® were employed for this study. Both MCF-7 and MCF-7R cell lines were cultured in DMEM-F12 containing *L*-glutamine (20 μM) and phenol red. KB cells were cultured in Eagle's minimum essential medium (EMEM) containing *L*-glutamine (20 μM), phenol red, and non-essential amino acid (5 ml). The media for all cell lines was supplemented with Gentamicin (500 units/ml; Life Technologies), 10% fetal calf serum, and it was standardized to give an iron concentration between 450 and 600 μg/100 g in order to reach the physiological iron levels in biological systems.[30] The cells were grown as monolayers in sterile, vented-capped, angle-necked cell culture flasks (Corning) and were maintained at 37°C in a humidified 5% $CO_2$ incubator (IR Autoflow Water-Jacketed Incubator; Jencons Nuaire) until confluent.

#### *4.3.1 Fluorescence pharmacokinetics and mechanistic study*

Cells were seeded into γ-sterilized 96-well plates (Orange Scientific, Triple Red Laboratory

Technologies) at a density of ~5 × $10^4$ per well for 48 h. The culture medium was removed and the cells were washed with PBS. The cells were incubated with freshly prepared solutions of ALA and ALA-HPOs derivatives: 100μL serum-free medium containing varying prodrugs concentrations was added to a designated series of wells. Each plate contained wells with cells without prodrug as control for subtracting the natural PpIX fluorescence reading. PpIX fluorescence induced by ALA and ALA-HPOs derivatives was measured from each well with a Perkin-Elmer LS 50B fluorescence spectrometer coupled to an automated plate reader (Perkin-Elmer) using 405 nm excitation and 635 nm emission wavelengths with slit widths set to 10 nm and the internal 515 nm long-pass filter used on the emission side. The spectral scans were recorded between 600 and 750 nm, discriminating PpIX from other porphyrins, should any be present. The mean fluorescence intensity (expressed in arbitrary units) was calculated after subtraction the control values. Time course measurements for PpIX fluorescence intensities were recorded with ALA or ALA-HPOs over periods of 2, 4, 6, and 24h with concentration varied between 1-100μM.

*Study on dependence of ALA transport on temperature.* Temperature dependent study was conducted for cellular uptake of prodrugs. MCF-7R and KB cells were seeded in two 96-well γ-irradiated plates, incubated for 48 h, and washed with PBS. ALA and ALA-HPOs prodrugs (500μM) in clear medium were added at 100μL/well and the plates were wrapped in foil. One plate was incubated at 37°C and the other at 4°C for 1h. The prodrugs were then removed, cells were rinsed in PBS, and 100μL clear medium was added to each well. The plates were both incubated at 37°C for 4 h to allow the ALA already taken up by the cells to be converted to PpIX. The amount of PpIX produced by the cells in the different conditions was evaluated as described above.

### *4.3.2 Photodynamic Treatment*

Cells were seeded into 96-well plates at a density of ~$5 \times 10^4$ per well. Following incubation for 48h, the cells were washed with PBS and 100µl solutions containing each compound at varying concentrations (between 1 µM – 100 µM) were added to their designated wells for set incubation periods. Each well plate contained three control wells without the compound and the compound at five different concentrations in triplicate. The plates were irradiated with a fluence of 2.5 J/cm$^2$ using a LumiSource lamp (PCI Biotech), which emits a uniform field of low-power blue light over an area of 14 × 32 cm. Peak output is ~420 nm, which overlaps with the PpIX Soret band. Immediately following irradiation, the medium was replaced and cells were incubated for further 18h. Cell cytotoxicity at 24 hr after treatment was determined using the 3-(4, 5-dimethylthiazol-2-yl)-2,5-diphenyltetrazolium bromide (MTT) assay: cells were incubated with medium containing MTT (1mg/mL dissolved in full DMEM-12 for MCF-7 and MCF-7R, EMEM for KB) for 2h. The insoluble end product (formazan derivatives) was dissolved in 100µL DMSO after removing the medium. Absorbance was quantified at 570nm nm using a 96-well plate reader (ELX800, BioTek Instruments). The mean cell survival was calculated for each prodrug at every concentration tested and expressed as a percentage of control cell survival values. Control wells contained cells without compounds and allocated in the same plate with the other compounds that were irradiated for phototoxicity experiments. For determination of 'dark' toxicity of the compounds, well plates were prepared in the same manner as above but without irradiation.

### *4.3.3 Determination of intracellular PpIX Content*

Cells were seeded into 100mm Petri-dishes at a density of $5 \times 10^4$ cells per well for 48 h at 37°C. The culture medium was removed and the cells were washed with PBS. The cells were then incubated with the 100µl of ALA or the selected ALA-HPO prodrugs for 4h, and then washed twice with PBS. CelLytic (Sigma-Aldrich) (1mL) was added and incubated for 15min at room temperature, and the cells were scraped and collected in cryostat vials. Cell extracts were centrifuged at 1800 *g* for 10 min to remove the cell debris, and the supernatant containing the PpIX was collected. The content of PpIX in the cell lysates was determined by a fluorescence plate reader (Perkin-Elmer) in 96 well plates, with excitation wavelength at 405nm and emission at wavelength at 635nm as reported above. The protein content of the cells was determined using a bicinchoninic acid protein determination kit (Sigma-Aldrich). We found that the final solution of the derivatized products, after acidic hydrolysis and derivatization was inhomogeneous, it was causing inconsistent result with HPLC analysis. Therefore, the ratio of acetylacetone solution was modified to increase the percentage of ethanol. The recovery of intracellular accumulation of ALA from ALA-HPOs was similar to ALA quantities after acidic hydrolysis, for one hour of incubation in KB and MCF-7R cell lines**.** Therefore, ester hydrolysis of the conjugates takes place rapidly and efficiently inside the cells. For all 6 × 24-well test plates the last three wells contained control cells not incubated with any compounds (blank controls). The PpIX fluorescence measurements from these wells were used to subtract the natural cellular PpIX auto-fluorescence from all the other measurements made from the same plate.

### *4.3.4 Intracellular ALA determination*

*Sample derivatisation and analysis procedures:* Stock solutions of ALA and ALA-HPO

conjugates in deionised water were prepared and stored at -20 °C. Working solutions were prepared daily by dilution of the stock solutions in media without phenol red or serum. Calibration samples were prepared by spiking blank cell lysate with the appropriate working solution. The acetylacetone reagent was prepared by mixing absolute ethanol, water, and acetylacetone in a 45/40/15 volumetric ratio. 10% formaldehyde was obtained by dilution of the commercially available 37% (v/v) aqueous solution in water. The solutions were stored at 4 °C. The derivatisation reactions were performed in a parallel synthesizer (Acteviotech) equipped with a 16-position reaction blocks. For the determination of ALA, the calibration samples were prepared by spiking 90µl of cell lysate with 10µl of the appropriate working solution. For the determination of ALA esters, 350µL of cell lysate was spiked with 50µl of the appropriate working solution. 200µl of such a mixture was diluted to 2 ml with 0.01M HCl in a 16 mm parallel synthesizer reaction tube. The tubes were transferred into the Greenhouse reactor preheated at 100 °C, refluxed for 3h under stirring, then cooled in an ice-bath. In an Acteviotech reaction tube equipped with a magnetic stirrer, 50 µL of calibration sample was added to 3500 µL of acetylacetone reagent and 450 µL of 10% formaldehyde solution. The tubes were placed in the parallel synthesizer reactor preheated at 100 °C, and stirred for 10 min. The reactor chamber was wrapped with foil in order to protect the tubes with the reaction mixture from light. The samples were then cooled in an ice-bath in the dark for 2 h, transferred into HPLC vials and kept in the auto-sampler at room temperature until the analysis was performed.

*HPLC fluorescence analysis:* HPLC analysis were performed on a Agilent system (Life Sciences & Chemical Analysis Group UK), following the published protocol with some modification.[49] The system consisted of a G1311A QuatPump fitted with an internal vacuum degasser, a WPS-

300SL analytical autosampler equipped H3BDSC10-H column compartment, a G132A FLD fluorescence detector. The separations were performed on a Gemini 5 µ C18 H3BDSC10-H column, 100 mm × 2.1 mm (Phenomenex, UK), equipped with a Security Guard C18 (ODS) 4 mm × 2.1mm ID guard column (Phenomenex, UK), at 35 ± 0.1 °C. The mobile phase consisted of 0.05% formic acid in water (solvent A) and 0.05% formic acid in methanol (solvent B). The composition of the mobile phase was as follows: 5.0–0.0 min at 40% solvent B, 0.0–7.0 min at 40% solvent B, 7.0–7.1 min 40–95% solvent B, 7.1–10.0 min at 95% solvent B, 10.0–10.1 min 95–40% solvent B. The flow rate was 0.5 mL/min. $\lambda_{exc}$ = 370 nm and $\lambda_{em}$ = 460 nm were used for the detection. For the low concentration range, 20 µl of sample were injected and the fluorescence detector was set on high sensitivity. For the high concentration range, 10 µl were injected and the detector was set on medium sensitivity. The peak corresponding to **1** eluted at 4.72 min. The total time required for the analysis was 12.1 min.

### *2.3.5 Statistical Analysis*

All data points and bars in the figures represent average values calculated from test solution concentrations being carried out in triplicate. The results were tabulated or graphically displayed with error bars representing the standard deviation (SD) of the mean. Data were analyzed using the unpaired Student's *t*-test, and results with $P < 0.05$ were considered significant.

## ASSOCIATED CONTENT

**Supporting Information.**

Molecular Formula Strings. This material is available free of charge via the Internet at

http://pubs.acs.org.

## AUTHOR INFORMATION

**Corresponding Author**

*(T.Z.) Phone: +86 571 28008976. E-mail: taozhou@zjgsu.edu.cn.

## ACKNOWLEDGMENT

The authors thank EPSRC (EP/G005087; EP/G004986; EP/G004382) and Zhejiang Provincial Natural Science Foundation of China (LY12B02014) and Science Technology Department of Zhejiang Province of China (No. 2013C24006) for the financial support.

## ABBREVIATIONS USED

ALA, 5-aminolaevulinic acid; HPO, 2-ethyl-3-hydroxypyridinone; DAD, diode array detector; DCC, dicyclohexylcarboimide; DFO, Desferrioxamine ; DMAP, 4-dimethylpyridylamine; *N*-Z-ALA, *N*-benzyloxycarbonyl-5-aminolevulinic acid; DIPAD, diisopropyl azodicarboxylate; MTT, 3-(4,5-dimethylthiazol-2-yl)-2,5- diphenyltetrazoliumbromide; PBS, phosphate buffered saline; PDT, Photodynamic therapy; PpIX, protoporphyrin IX; EDTA, ethylenediamine tetraacetic acid.

## REFERENCES

(1) Juzeniene, A.; Peng, Q,; Moan, J. Milestones in the development of photodynamic therapy and fluorescence diagnosis. *Photochem. Photobiol. Sci.* **2007**, *6*, 1234-1245.

(2) Snow, G. B.; van Dongen, G. A. Basic principles, applications in oncology and improved selectivity of photodynamic therapy. *Anticancer Res.* **2003**, *23*, 505–522.

(3) De Rosa, F. S.; Bentley, M. V. Photodynamic therapy of skin cancers: sensitizers, clinical studies and future directives. *Pharm. Res.* **2000**, *17*, 1447-1455.

(4) Ochsner, M. Photophysical and photobiological processes in the photodynamic therapy of tumours. *J. Photochem.Photobiol.* **1997**, *39*, 1-18.

(5) Kennedy, J. C.; Marcus, S. L.; Pottier, R. H. Photodynamic therapy (PDT) and photodiagnosis (PD) using endogenous photosensitization induced by 5-aminolevulinic acid (ALA): mechanisms and clinical results, *J. Clin. Laser Med. Surg.* **1996**, *14*, 289–304.

(6) Peng, Q.; Warloe, T.; Berg, K.; Moan, J.; Kongshaug, M.; Giercksky, K. E.; Nesland, J. M. 5-Aminolevulinic acid-based photodynamic therapy. Clinical research and future challenges. *Cancer* **1997**, *79*, 2282-2308.

(7) Lopez, R. F. V.; Lange, N.; Guy, R.; Bentley, M. V. Photodynamic therapy of skin cancer: controlled drug delivery of 5-ALA and its esters. *Adv. Drug Deliv. Rev.* **2004**, *56*, 77-94.

(8) Horn, M.; Wolf, P.; Wulf, H. C.; Warloe, T.; Fritsch, C.; Rhodes, L. E.; Kaufmann, R.; De Rie, M.; Legat, F. J.; Stender, I. M.; Soler, A. M.; Wennberg, A. M.; Wong, G. A. E.; Larko, O. Topical methyl aminolaevulinate photodynamic therapy in patients with basal cell carcinoma prone to complications and poor cosmetic outcome with conventional treatment. *Br. J. Dermatol.* **2003**, *149*, 1242–1249.

(9) Rhodes, L.E.; de Rie, M.; Enstrom, Y.; Groves, R.; Morken, T.; Goulden, V.; Wong, G. A.; Grob, J. J.; Varma, S.; Wolf, P. Photodynamic therapy using topical methyl aminolevulinate vs surgery for nodular basal cell carcinoma: Results of a multicenter randomized prospective trial. *Arch. Dermatol.* **2004**, *140*, 17–23.

(10) Yoon, J. H.; Yoon, H. E.; Kim, O.; Kim, S. K.; Ahn, S. G.; Kang, K. W. The enhanced anti-cancer effect of hexenyl ester of 5-aminolaevulinic acid photodynamic therapy in

adriamycin-resistant compared to non-resistant breast cancer cells. *Laser. Surg. Med.* **2012**, *44*, 76-86.

(11) Uehlinger, P.; Zellweger, M.; Wagnières, G.; Juillerat-Jeanneret, L.; van den Bergh, H.; Lange, N. 5-Aminolevulinic acid and its derivatives: physical chemical properties and protoporphyrin IX formation in cultured cells. *J. Photochem. Photobiol. B* **2000**, *54*, 72-80.

(12) Whitaker, C.; Battah, S.; Edwards, C.; Boyle, R.; Mattews, E. K. Photosensitization of pancreatic tumour cells by delta-aminolevulinic acids esters. *Anti-Cancer Drug Des.* **2000**, *15*, 161-170.

(13) Battah, S.; O'Nell, S.; Edwards, C.; Balaratnam, S.; Dobbin, P.; MacRobert, A. J. Enhanced porphyrin accumulation using dendritic derivatives of 5-aminolaevulinic acid for photodynamic therapy: An in vitro study. *Int. J. Biochem. Cell Biol.* **2006**, *38*, 1382-1392.

(14) Babič, A.; Herceg, V.; Ateb, I.; Allémann, E.; Lange, N. Tunable phosphatase-sensitive stable prodrugs of 5-aminolevulinic acid for tumor fluorescence photodetection. *J. Control. Release* **2016**, *235*, 155–164.

(15) Berkovitch, G.; Doron, D.; Nudelman, A.; Malik, Z.; Rephaeli, A. Novel multifunctional acyloxyalkyl ester prodrugs of 5-aminolevulinic acid display improved anticancer activity independent and dependent on photoactivation. *J. Med. Chem.* **2008**, *51*, 7356-7369.

(16) Bourre, L.; Giuntini, F.; Eggleston, I. M.; Wilson, M.; MacRobert, A. J. 5-Aminolaevulinic acid peptide prodrugs enhance photosensitization for photodynamic therapy. *Mol. Cancer Ther.* **2008**, *7*, 1720–1729.

(17) Giuntini, F.; Bourré, L.; MacRobert, A. J.; Wilson, M.; Eggleston, I. M. Improved peptide prodrugs of 5-ALA for PDT: rationalization of cellular accumulation and protoporphyrin IX

production by direct determination of cellular prodrug uptake and prodrug metabolization. *J. Med. Chem.* **2009**, *52*, 4026–4037.

(18) Di Venosa, G.; Vallecorsa, P.; Giuntini, F.; Mamone, L.; Batlle, A.; Vanzuli, S.; Juarranz, A.; MacRobert, A. J.; Eggleston, I. M.; Casas, A. The use of dipeptide derivatives of 5-aminolaevulinic acid promotes their entry to tumor cells and improves tumor selectivity of photodynamic therapy. *Mol. Cancer Ther.* **2015**, *14*, 440–451.

(19) Konan, Y.N.; Gurny, R.; Allemann, E. State of the art in the delivery of photosensitizers for photodynamic therapy. *J. Photochem. Photobiol. B* **2002**, *66*, 89–106.

(20) Peng, Q.; Moan, J.; Warloe, T.; Iani, V.; Steen, H. B.; Bjorseth, A.; Nesland, J. M. Build-up of esterified aminolevulinic-acid-derivative-induced porphyrin fluorescence in normal mouse skin. *J. Photochem. Photobiol. B* **1996**, *34*, 95-96.

(21) Peng, Q.; Berg, K.; Moan, J.; Kongshaug, M.; Nesland, J. M. 5-Aminolevulinic acid-based photodynamic therapy: principles and experimental research. *Photochem. Photobiol.* **1997**, *65*, 235–251.

(22) Gardner, L. C.; Smith, S. J.; Cox, T. M. Biosynthesis of delta-aminolevulinic acid and the regulation of heme formation by immature erythroid cells in man. *J. Biol. Chem.* **1991**, *266*, 22010–22018.

(23) Hanania, J.; Malik, Z. The effect of EDTA and serum on endogenous porphyrin accumulation and photodynamic sensitization of human K562 leukemic cells. *Cancer Lett.* **1992**, *65*, 127–131.

(24) Liu, H. F.; Xu, S. Z.; Zhang, C. R. Influence of CaNa2 EDTA on topical 5-aminolaevulinic acid photodynamic therapy. *Chin. Med. J.* **2004**, *117*, 922–926.

(25) Barr, H.; Kendall, C.; Bazant-Hegemark, F.; Moayyedi, P.; Shetty, G.; Stone, N. Endoscopic screening and surveillance for Barrett's esophagus--clinical implications. *MedGenMed* **2006**, *8*, 88.

(26) Yang, J.; Xia, Y.; Liu, X.; Jiang, S.; Xiong, L. Desferrioxamine shows different potentials for enhancing 5-aminolaevulinic acid-based photodynamic therapy in several cutaneous cell lines. *Lasers Med Sci.* **2010**, *25*, 251-257.

(27) Pourzand, C.; Reelfs, O.; Kvam, E.; Tyrrell, R. M. The iron regulatory protein can determine the effectiveness of 5-aminolevulinic acid in inducing protoporphyrin IX in human primary skin fibroblasts. *J. Invest. Dermatol.* **1999**, *112*, 419–425.

(28) Bech, O.; Phillips, D.; Moan, J.; MacRobert, A. J. A hydroxypyridinone (CP94) enhances protoporphyrin IX formation in 5-aminolaevulinic acid treated cells. *J. Photochem. Photobiol. B* **1997**, *41*, 136–144.

(29) Chang, S. C.; MacRobert, A. J.; Porter J. B.; Bown, S. G. The efficacy of an iron chelator (CP94) in increasing cellular protoporphyrin IX following intravesical 5-aminolaevulinic acid administration: an in vivo study. *J. Photochem. Photobiol. B* **1997**, *38*, 114–122.

(30) Curnow, A.; MacRobert, A. J.; Bown, S. G. Comparing and combining light dose fractionation and iron chelation to enhance experimental photodynamic therapy with aminolevulinic acid. *Laser. Surg. Med.* **2006**, *38*, 325–331.

(31) Curnow, A.; McIlroy, B. W.; Postle-Hacon, M. J.; Porter, J. B.; MacRobert, A. J.; Bown, S. G. Enhancement of 5-amino-laevulinic acid-induced photodynamic therapy in normal rat colon using hydroxypyridinone iron-chelating agents. *Br. J. Cancer* **1998**, *78*, 1278–1282.

(32) Dobbin, P. S.; Hider, R. C.; Hall, A. D.; Taylor, P. D.; Sarpong, P.; Porter, J. B.; Xiao, G.; van der Helm, D. Synthesis, physicochemical properties, and biological evaluation of N-

substituted 2-alkyl-3-hydroxy-4(1H)-pyridinones: orally active iron chelators with clinical potential. *J. Med. Chem.* **1993**, *36*, 2448-2458.

(33) Hershko, C.; Link, G.; Pinson, A.; Peter, H. H.; Dobbin, P.; Hider, R. C. Iron mobilization from myocardial cells by 3-hydroxypyridin-4-one chelators: studies in rat heart cells in culture. *Blood* **1991**, *77*, 2049-2053.

(34) Porter, J. B.; Gyparaki, M.; Burke, L. C.; Huehns, E. R.; Sarpong, P.; Saez, V.; Hider, R. C. Iron mobilization from hepatocyte monolayer cultures by chelators: The importance of membrane permeability and the iron-binding constant. *Blood* **1988**, *72*, 1497–1503.

(35) Smith, A. G.; Clothier, B.; Francis, J. E.; Gibbs, A. H.; De Matteis, F.; Hider, R. C. Protoporphyria induced by the orally active iron chelator 1,2-diethyl-3-hydroxypyridin-4-one in C57BL/10ScSn mice. *Blood* **1997**, *89*, 1045–1051.

(36) Zhu, C. F.; Battah, S.; Kong, X. L.; Reeder, B. J.; Hider, R. C.; Zhou, T. Design, Synthesis and biological evaluation of 5-aminolaevulinic acid/3-hydroxypyridinone conjugates as potential photodynamic therapeutical Agents. *Bioorg. Med. Chem. Lett.* **2015**, *25*, 558–561.

(37) Zhou, T.; Shao, L. L.; Battah, S.; Zhu, C. F.; Hider, R. C.; Reeder, B. J.; Jabeen, A.; MacRobert, A. J.; Ren, G. R.; Liang, X. L. Design and synthesis of 5-aminolaevulinic Acid/3-hydroxypyridinone conjugates for photodynamic therapy: enhancement of protoporphyrin IX production and photo-toxicity in tumor cells. *MedChemComm* **2016**, 7, 1190-1196.

(38) Hoyes, K. P.; Porter, J. B. Subcellular-distribution of desferrioxamine and hydroxypyridin-4-one chelators in K562 cells affects chelation of intracellular iron pools. *Brit. J. Haematol.* **1993**, *85*, 393-400,

(39) Xie, Y. Y.; M. S.; Hu, P. P.; Kong, X. L.; Qiu, D. H.; Xu, J. L.; Hider, R. C.; Zhou, T. Synthesis, physico-chemical properties, an antimicrobial evaluation of a new series of iron(III) hexadentate chelators. *Med. Chem. Res.* **2013**, *22*, 2351-2359.

(40) Feuerstein, T.; Berkovitch-Luria, G.; Nudelman, A.; Rephaeli, A.; Malik, Z. Modulating ALA-PDT efficacy of mutlidrug resistant MCF-7 breast cancer cells using ALA prodrug. *Photochem. Photobiol. Sci.* **2011**, *10*, 1926-1933.

(41) Wu, R. W.; Chu, E. S.; Yow, C. M.; Chen, J. Y. Photodynamic effects on nasopharyngeal carcinoma (NPC) cells with 5-aminolevulinic acid or its hexyl ester. *Cancer Lett.* **2006**, *242*, 112-119.

(42) Jerjes, W.; Upile, T.; Hamdoon, Z.; Mosse, C. A.; Akram, S.; Hopper, C. Photodynamic therapy outcome for oral dysplasia. *Lasers Surg. Med.* **2011**, *43*, 192-199.

(43) Dogra, Y.; Ferguson, D. C. J.; Dodd, N. J. F.; Smerdon, G. R.; Curnow, A.; Winyard, P. G. The hydroxypyridinone iron chelator CP94 increases methyl-aminolevulinate-based photodynamic cell killing by increasing the generation of reactive oxygen species. *Redox Biol.* **2016**, *9,* 90–99.

(44) De Rosaa, F.; Tedescob, A.; Lopez, R.; Pierre, M.; Lange, M.; Marchetti, J.; Gomes, J. In vitro skin permeation and retention of 5-aminolevulinic acid ester derivatives for photodynamic therapy. *J. Control. Release* **2003**, *89*, 261–269.

(45) Rodriguez, L.; Batlle, A.; Di Venosa, G.; Battah, S.; Dobbin, P.; MacRobert, A. J.; Casas, A. Mechanisms of 5-aminolevulinic acid ester uptake in mammalian cells. *Br. J. Pharmacol.* **2006**, *147*, 825-833.

(46) Curnow, A.; Pye, A. The importance of iron chelation and iron availability during PpIX-induced photodynamic therapy. *Photonics Lasers Med.* **2015**, *4,* 39–58.

(47) Di Venosa, G. M.; Casas, A. G.; Battah, S.; Dobbin, P.; Fukuda, H.; MacRobert, A. J.; Batlle, A. Investigation of a novel dendritic derivative of 5-aminolaevulinic acid for photodynamic therapy. *Int. J. Biochem. Cell Biol.* **2006**, *38*, 82-91.

(48) Giuntini, F.; Bourré, L.; MacRobert, A. J.; Wilson, M.; Eggleston, I. M. Quantitative determination of 5- aminolaevulinic acid and its esters in cell lysates by HPLC-fluorescence. *J. Chromatogr. B* **2008**, *875*, 562–566.

(49) Dixon, M. B.; MacRobert, A. J.; Eggleston, I. M. Novel prodrug approach to photodynamic therapy: Fmoc solid-phase synthesis of a cell permeable peptide incorporating 5-aminolaevulinic acid. *Bioorg. Med. Chem. Lett.* **2007**, *17*, 4518-4522.

TABLES

**Table 1.** Clog*P* and $LD_{50}$ values of ALA, ALA-HPO conjugates and ALA esters.

| Compounds | $LD_{50}$ (μM) | | | Clog*P* |
|---|---|---|---|---|
| | KB | MCF-7 | MCF-7R | |
| ALA | 124.0 ± 5.2 | 131.2 ± 7.4 | 122.5 ± 8.2 | -1.3 |
| **7a** | 114.6 ± 3.6 | 124.2 ± 5.3 | 122.4 ± 5.6 | -1.96 |
| **7b** | 65.1 ± 6.3 | 76.5 ± 7.1 | 61.2 ± 3.9 | -1.42 |
| **7c** | 5.2 ± 2.5 | 13.4 ± 2.6 | 8.1 ± 4.6 | -0.41 |
| **7d** | 3.1 ± 1.1 | 10.9 ± 3.2 | 4.2 ± 2.2 | 0.60 |
| **7e** | 2.3 ± 0.5 | 8.1 ± 4.1 | 3.9 ± 2.4 | 0.73 |
| **7f** | 2.5 ± 0.32 | 12.9 ± 2.6 | 5.5 ± 3.1 | 0.91 |
| **12** | 24.1 ±1.42 | 16.6 ± 4.4 | 8.4 ± 2.4 | -1.28 |
| **18** | 107.5 ± 4.6 | 113.3 ± 6.5 | 104.5 ± 5.1 | -1.65 |
| **23** | 19.6 ± 1.4 | 15.8 ± 5.1 | 11.3 ± 3.8 | -2.37 |
| **24** | 2.6 ± 0.26 | 9.3 ± 0.07 | 8.4 ± 0.12 | 0.83 |
| **25** | ND | ND | ND | 1.84 |

Notes: Clog*P* values were obtained using an internet software (http://www.molinspiration.com/cgi-bin/properties). $LD_{50}$ values were calculated from two sets of phototoxicity experiments in KB, MCF-7 and MCF-7R cell lines after 4 h incubation using concentrations between 20-100 μM for (**ALA, 7a, 7b, 12** and **23**) and concentrations between 2-10 μM for (**7c, 7d, 7e** and **7f**) prodrugs and irradiated with 2.5 J/$cm^2$.

**Chart 1. Structures of ALA-HPO conjugates and ALA esters**

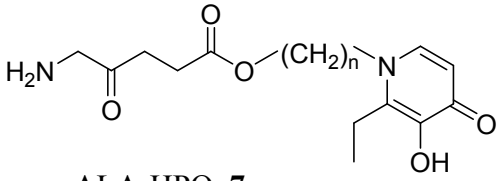

ALA-HPO **7**

**7a**: n = 2; **7b**: n = 4; **7c**: n = 6;
**7d**: n = 8; **7e**: n = 10; **7f**: n = 12

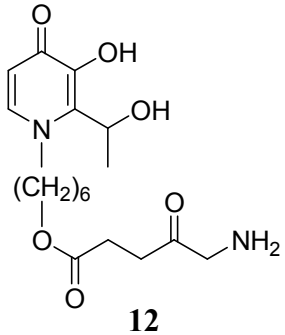

**12**

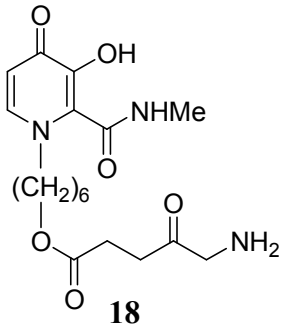

**18**

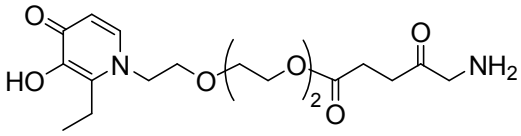

**23**

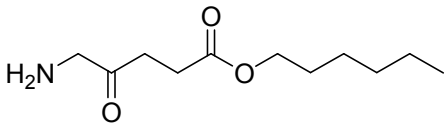

hexyl ALA (**24**)

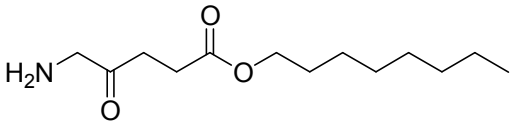

octyl ALA (**25**)

**Figure captions**

**Figure 1.** PpIX fluorescence intensity recorded in the MCF-7R cell line after exposure to different concentrations of ALA or ALA-HPOs or hexyl and octyl ALA ester prodrugs. The results were obtained after 6 h incubation at 37°C.

**Figure 2.** PpIX fluorescence time course in KB cell line after exposure to ALA (50 μM) or ALA-HPO prodrugs (50 μM). Cells were incubated at 37 °C in a $CO_2$ humidified incubator.

**Figure 3.** PpIX fluorescence produced by ALA or ALA-HPO prodrugs (500μM), KB cells pre-incubated at 4°C/1h and cells incubated only at 37°C/1h, then both were further incubated at 37°C for 4h, humidified with 5% $CO_2$.

**Figure 4.** (A) PpIX fluorescence production recorded in MCF-7 and MCF-7R cell lines after exposure to different ALA-HPOs (50 μM) in comparison to PpIX fluorescence produced by incubation of 50 μM ALA and HPOs as a 1:1 mixture. The results were obtained after 6 h incubation at 37 °C. (B) Time-course profile of PpIX fluorescence production recorded in KB cells after exposure to 100μM ALA, ALA-HPOs conjugates or (ALA + HPO) mixture incubated at 37°C. **5c**: 2-ethyl-3-hydroxy-1-(6-hydroxyhexyl)pyridin-4(1H)-one; **5d**: 2-ethyl-3-hydroxy-1-(8-hydroxyoctyl)pyridin-4(1*H*)-one; **5e**: 2-ethyl-3-hydroxy-1-(10-hydroxydecyl)pyridin-4(1H)-one; **5f**: 2-ethyl-3-hydroxy-1-(12-hydroxydodecyl)pyridin-4(1*H*)-one; **21b**: 1-(2-(2-(2-hydroxyethoxy)ethoxy)ethyl)-2-ethyl-3-hydroxypyridin-4(1H)-one.

**Figure 5.** Phototoxicity over a range of ALA and ALA-HPO concentrations after 4 h incubation with the KB cell line, irradiated by 2.5 J/cm$^2$ blue light.

**Figure 6.** Dark toxicity of ALA, ALA-HPOs, and hexyl-ALA in KB cells incubated for 4h without irradiation, then continued for 24h after removal of the prodrugs.

**Figure 7.** (A) Chemically extracted cellular concentrations per mg protein of intracellular ALA or ALA-HPOs with celLytic after 2h incubation at 100 μM. (B) PpIX cellular concentrations per mg protein measured at 24 h by chemical extraction using celLytic following 2h incubation with ALA and ALA-HPO conjugates at 37 °C.

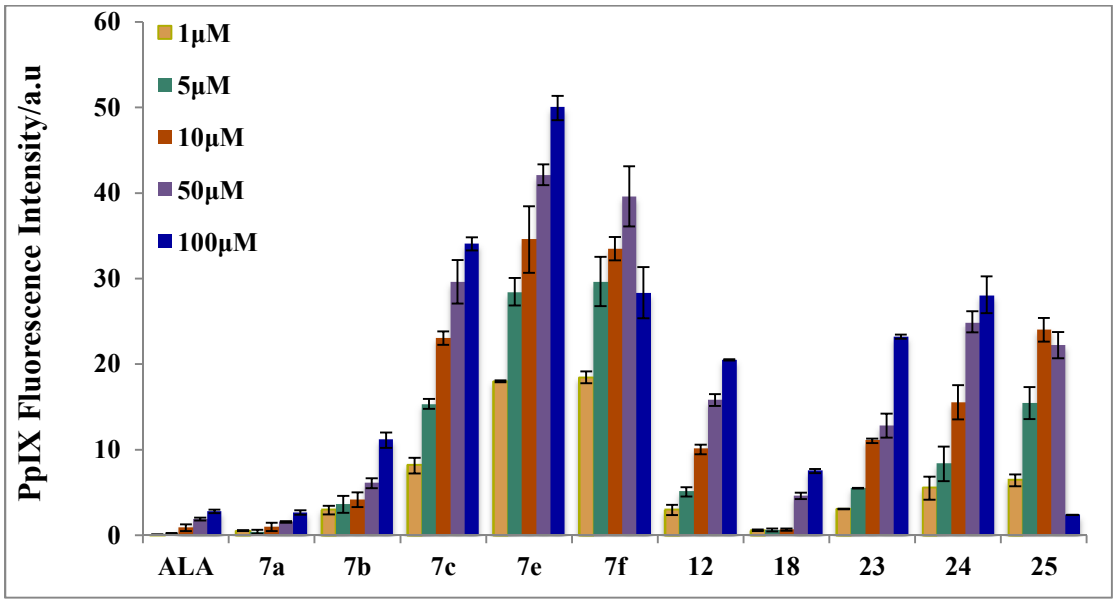
PpIX Fluorescence Intensity/a.u
60
50
40
30
20
10
0
1μM
5μM
10μM
50μM
100μM
ALA
7a
7b
7c
7e
7f
12
18
23
24
25

**Figure 1**

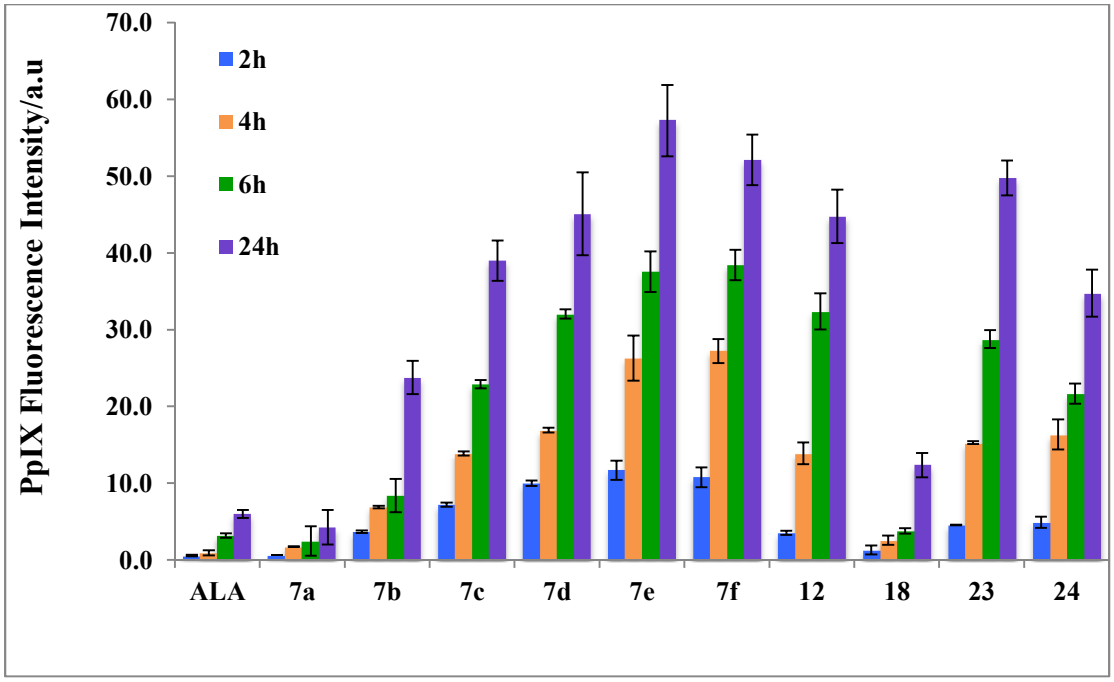
PpIX Fluorescence Intensity/a.u
70.0
60.0
50.0
40.0
30.0
20.0
10.0
0.0
2h
4h
6h
24h
ALA
7a
7b
7c
7d
7e
7f
12
18
23
24

**Figure 2**

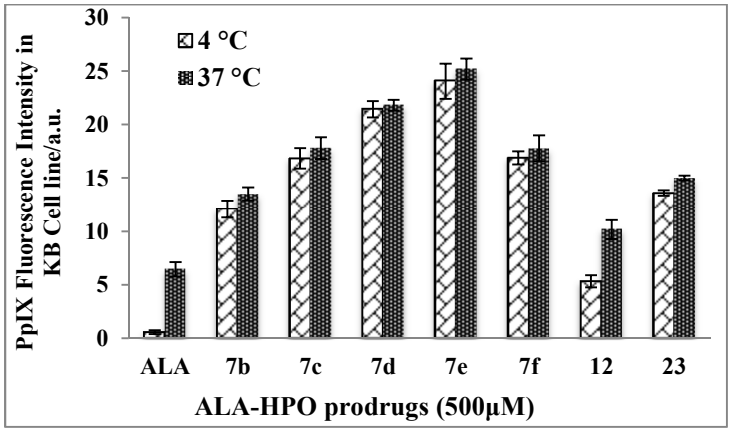
PpIX Fluorescence Intensity in KB Cell line/a.u.
30
25
20
15
10
5
0
4 °C
37 °C
ALA
7b
7c
7d
7e
7f
12
23
ALA-HPO prodrugs (500μM)

**Figure 3.**

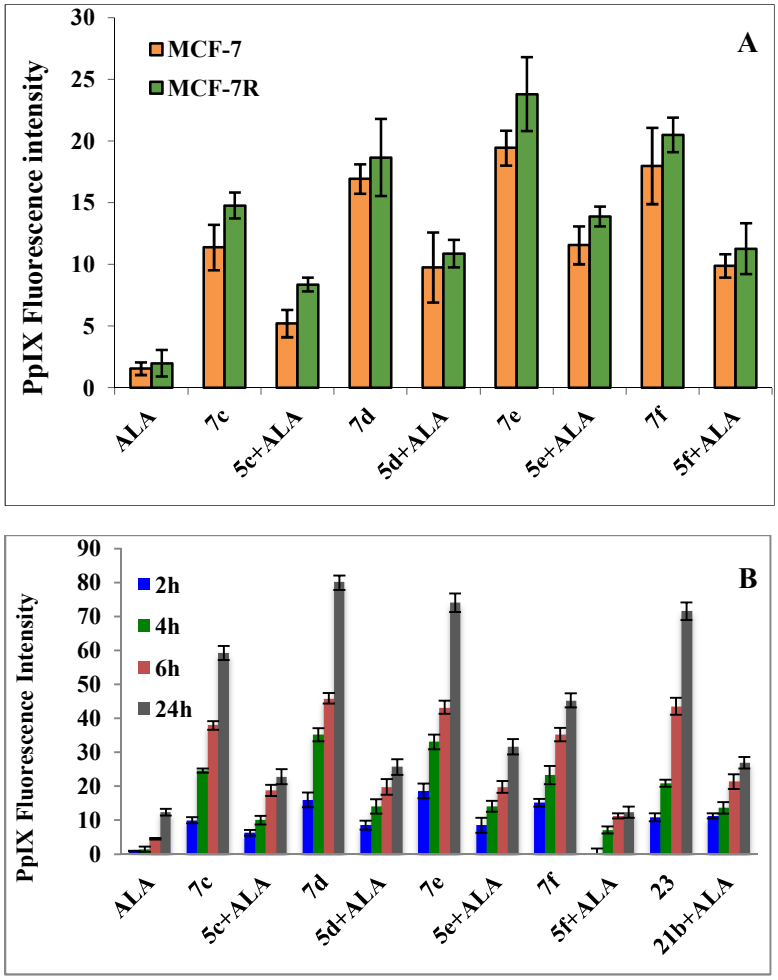
A
MCF-7
MCF-7R
PpIX Fluorescence intensity
30
25
20
15
10
5
0
ALA
7c
5c+ALA
7d
5d+ALA
7e
5e+ALA
7f
5f+ALA
B
2h
4h
6h
24h
PpIX Fluorescence Intensity
90
80
70
60
50
40
30
20
10
0
ALA
7c
5c+ALA
7d
5d+ALA
7e
5e+ALA
7f
5f+ALA
23
21b+ALA

**Figure 4**

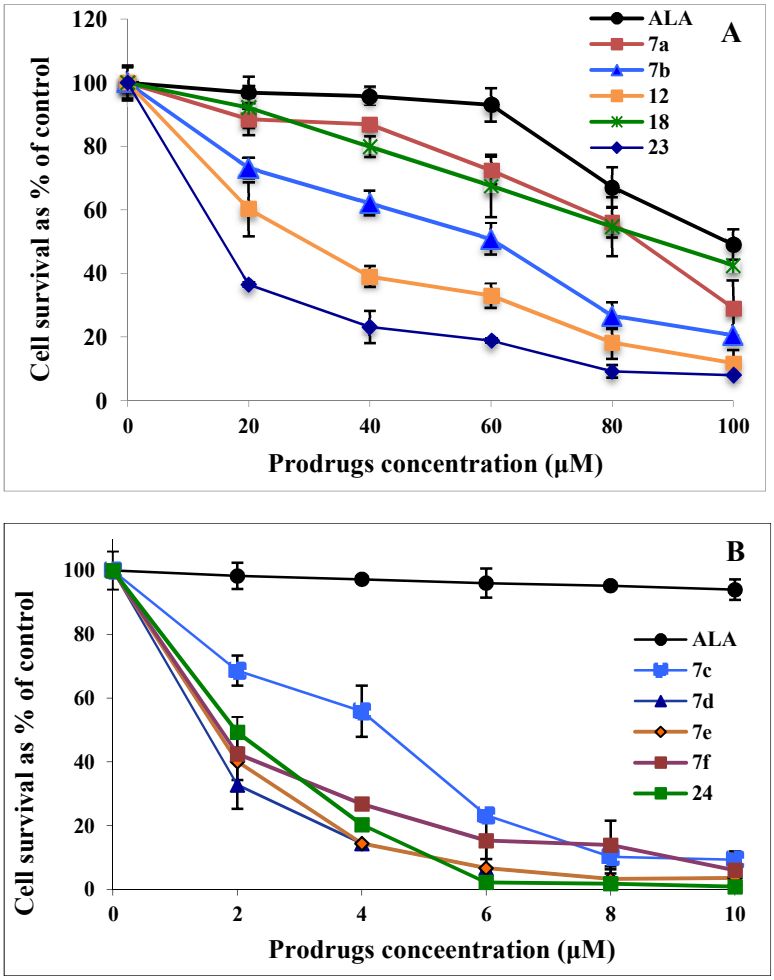
A
ALA
7a
7b
12
18
23
Cell survival as % of control
Prodrugs concentration (μM)
B
ALA
7c
7d
7e
7f
24
Cell survival as % of control
Prodrugs conceentration (μM)

**Figure 5.**

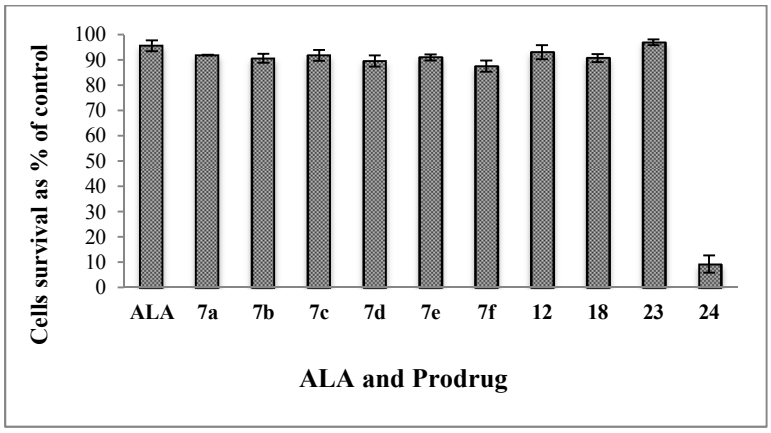
Cells survival as % of control
100
90
80
70
60
50
40
30
20
10
0
ALA
7a
7b
7c
7d
7e
7f
12
18
23
24
ALA and Prodrug

**Figure 6.**

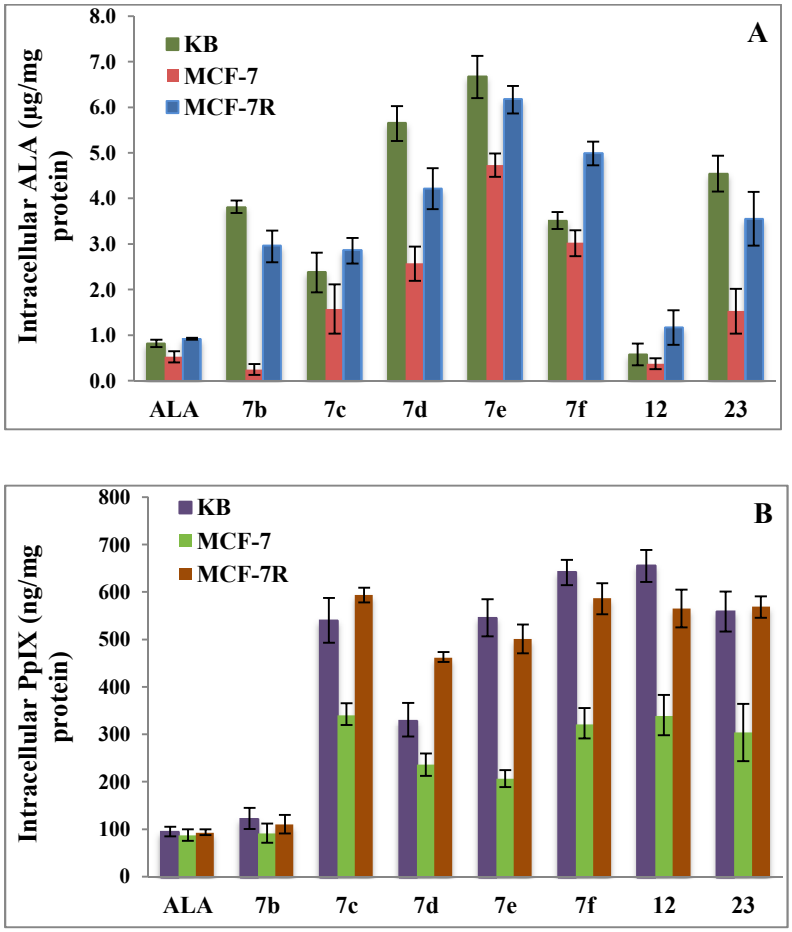
A
KB
MCF-7
MCF-7R
Intracellular ALA (µg/mg protein)
8.0
7.0
6.0
5.0
4.0
3.0
2.0
1.0
0.0
ALA
7b
7c
7d
7e
7f
12
23
B
KB
MCF-7
MCF-7R
Intracellular PpIX (ng/mg protein)
800
700
600
500
400
300
200
100
0
ALA
7b
7c
7d
7e
7f
12
23

**Figure 7.**

## Schemes

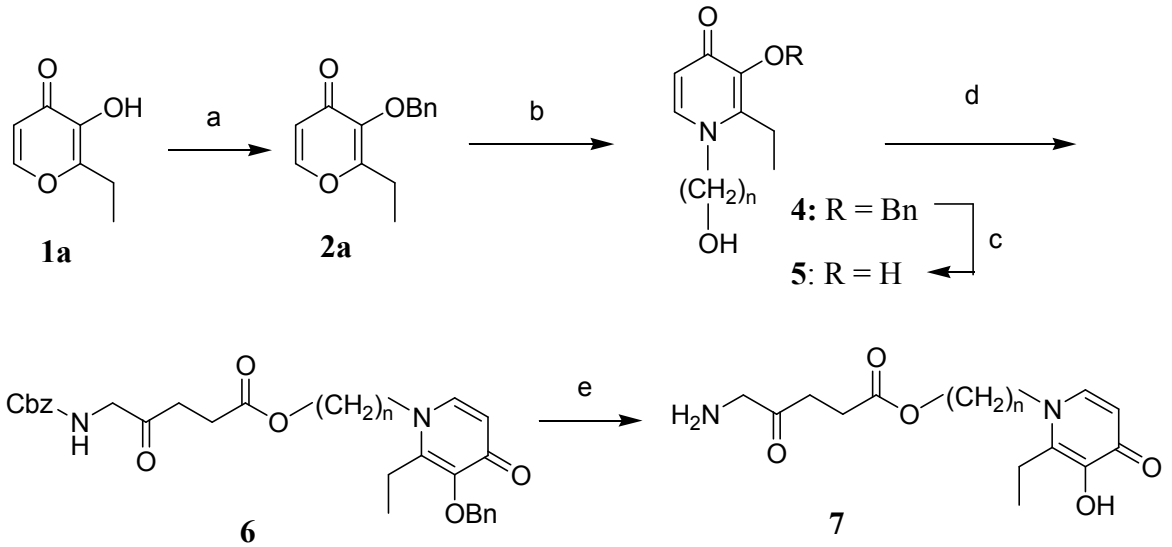


**Scheme 1**

**Scheme 1.** Synthesis of ALA-HPO conjugates **7**. (a) BnCl; (b) $NH_2(CH_2)_nOH$ (**3**); (c) $H_2$, Pd/C, MeOH; (d) *N*-Cbz-ALA (**7**), DCC, DMAP; e) $H_2$, Pd/C, EtOAc/MeOH.

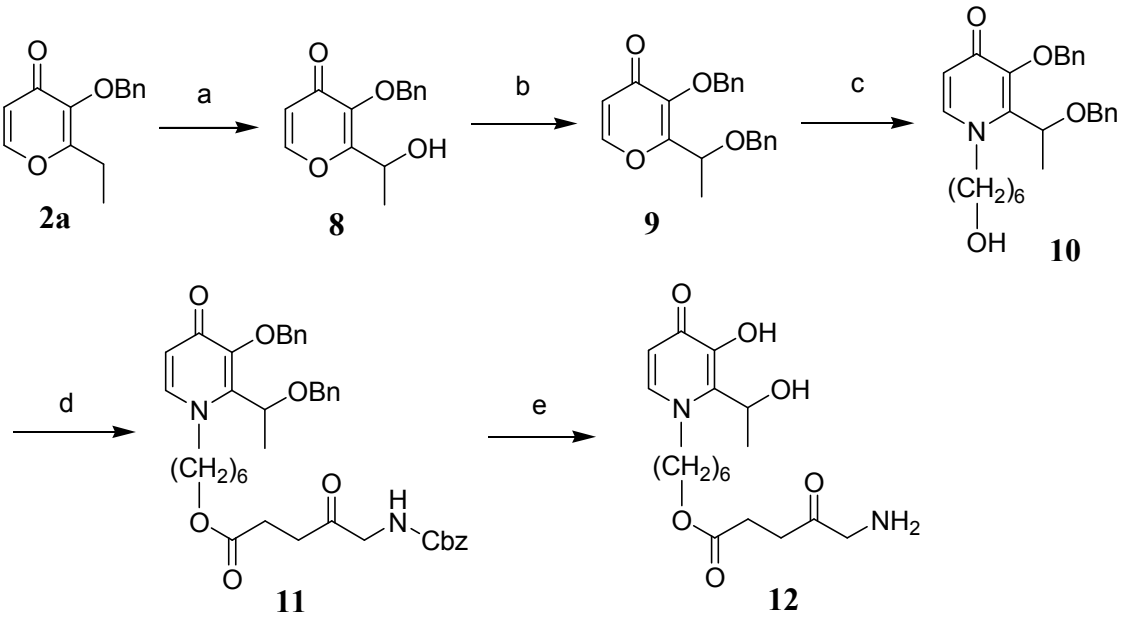


**Scheme 2**

**Scheme 2.** Synthesis of ALA-HPO conjugate **12**. (a) $SeO_2$; (b) BnBr; (c) $NH_2(CH_2)_6OH$; (d) *N*-Cbz-ALA (**7**), DCC, DMAP; (e) $H_2$, Pd/C.

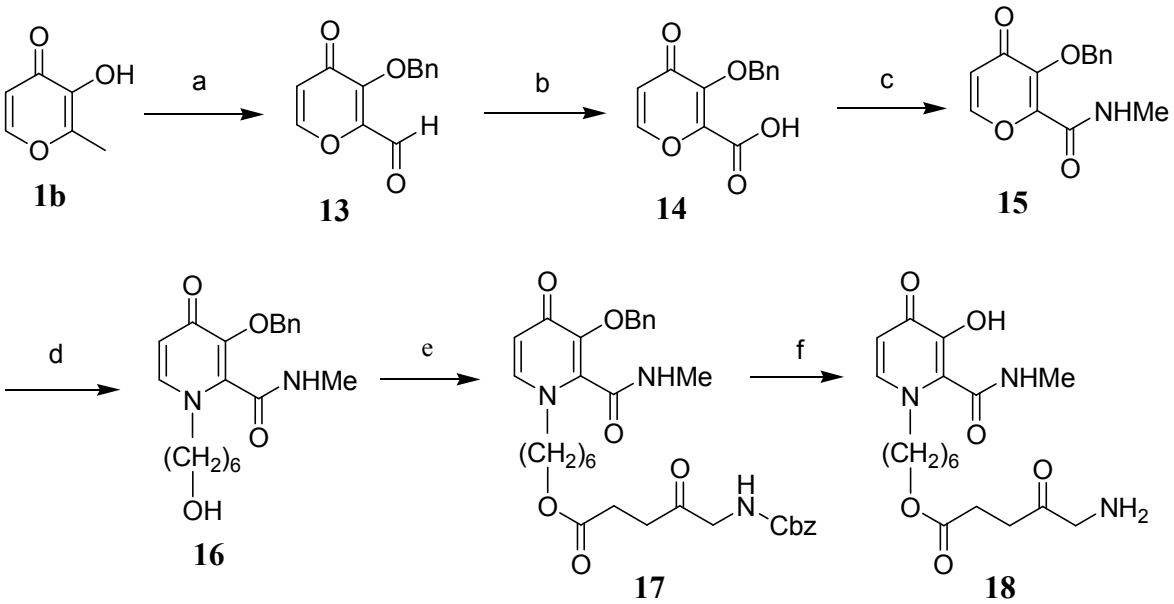


**Scheme 3**

**Scheme 3.** Synthesis of ALA-HPO conjugate **18**. (a) i) BnCl, ii) $SeO_2$; (b) $NH_2SO_3H$, $NaClO_2$; (c) i) DCC, NHS, ii) $MeNH_2$; (d) $NH_2(CH_2)_6OH$; (e) *N*-Cbz-ALA (**7**), DCC, DMAP; (f) $H_2$, Pd/C.

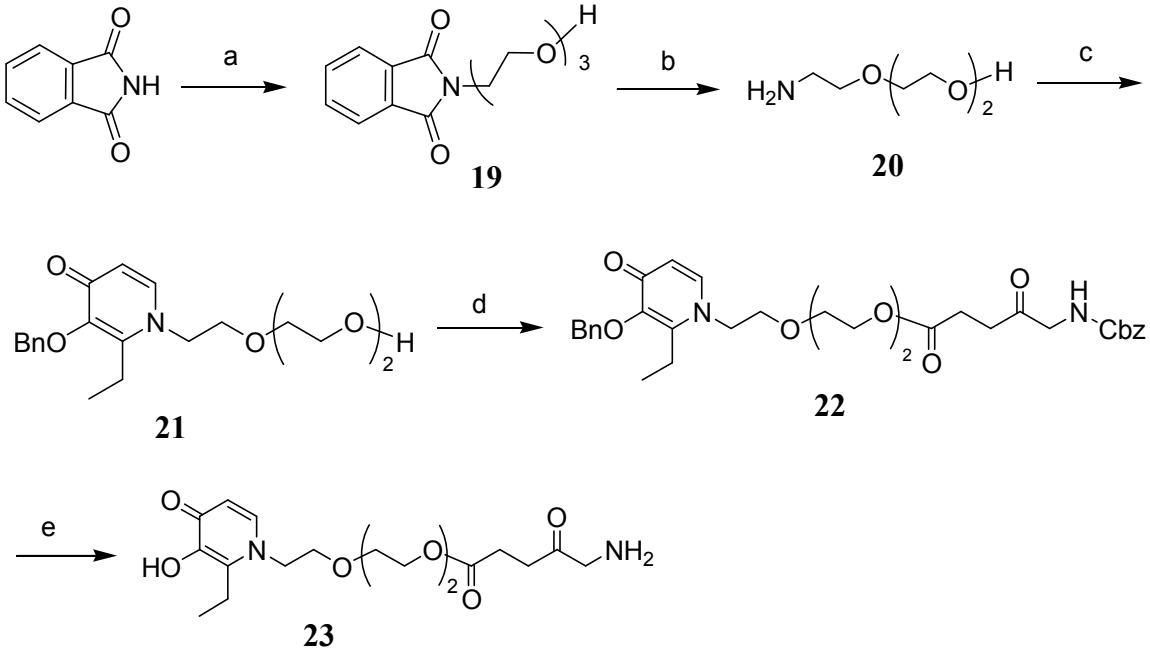


**Scheme 4**

**Scheme 4.** Synthesis of ALA-HPO conjugate **23**. (a) $HO(CH_2CH_2O)_3H$, $Ph_3P$, DIPAD; (b) $NH_2NH_2$; (c) **2a**; (d) *N*-Cbz-ALA (**7**), DCC, DMAP; (e) $H_2$, Pd/C.

# Table of Contents Graphic